www.ias.is

ISSN 2298-786X

Icelandic Agricultural Sciences

37 / 2024

Icelandic Agricultural Sciences

Icel. Agric. Sci.

www.ias.is

Published by:

Agricultural University of Iceland (Landbúnaðarháskóli Íslands)
Marine and Freshwater Research Institute (Hafrannsóknastofnun, rannsókna- og ráðgjafastofnun hafs og vatna)
Institute for Experimental Pathology, University of Iceland (Keldur, Tilraunastöð Háskóla Íslands í meinafræði)
Land and Forest Iceland (Land og Skógur)
Matís, Ltd. – Icelandic Food and Biotech R&D Institute (Matís ohf. – Þekkingar- og rannsóknarfyrirtæki í þróun og nýsköpun í matvælaiðnaði, líftækni og matvælaöryggi**)**
The Icelandic Agricultural Advisory Centre (Ráðagjafamiðstöð Landbúnaðarins)

Contact and submission

Björn Thorsteinsson at *editor@ias.is*

Cover Photo: Sheep grazing at Agricultural Universtiy of Iceland experimental sheep farm
Photograper: Eyjólfur Kristinn Örnólfsson

ICELANDIC AGRICULTURAL SCIENCES 37 / 2024

CONTENTS

Editorial

The 2024 IAS issue includes four contributions, and as usual on diverse topics of applied life sciences that are relevant under boreal, alpine, arctic or subarctic conditions which defines the scopeof our journal.

The first publication is about studies on immunological tissue is present in the rostral oral cavity of icelandic horses indicating the possibility of application of antigens in allergen-specific immunotherapy via the oral mucosa. The second publication is on tree-ring width and stable isotope analyses of *Picea sitchensis* from Iceland revealing growth potential under predicted climate change. The third publication is on models for simulating the temporal development of black cottonwood plantations in Iceland. The fourth publication is about studies on the relationship between live weight and body condition score and estimation of standard reference weight of ewes from the Icelandic sheep breed based on data collected for 22 years at the Agricultural Universtiy of Iceland's experimental sheepfarm.

The IAS Editorial Board decided last year that, starting with the 2025 issue, the journal's name would be expanded to include an environmental reference in the name and become Icelandic Agricultural and Environmental Sciences. The journal's defined scope has retained the environmental element since the beginning, but it has been missing from the title, which will now be added.

The editorial board hopes that the expansion of the name will appeal even more to authors who are engaged in environmental research that falls within the journal's scope.

Björn Thorsteinsson
Editor in Chief

www.ias.is
https://doi.org/10.16886/IAS.2024.01 ICEL. AGRIC. SCI. 37 (2024), 3-9

Well-developed immunological tissue is present in the rostral oral cavity of horses as revealed by histological and immunohistochemical examination

Ólöf Guðrún Sigurðardóttir[1]*, Einar Jörundsson[1‡], Vilhjálmur Svansson[1], Eygló Gísladóttir[1], Lauren Tryggvason[2] and Sigurbjörg Torsteinsdóttir[1]

[1]Institute for Experimental Pathology at Keldur, University of Iceland, Keldnavegur 3, IS-112 Reykjavik, Iceland.
Email: olof@hi.is, vsvanss@hi.is, eyglog@gmail.com, sibbath@hi.is
[2]Emerson & Watson Equine Veterinary Surgeons, 5 Cheapside Court, Sunninghill Road, Ascot, United Kingdom, SL5 7RF.
Email: lauren@emerson-watson.com

‡ *Deceased*

ABSTRACT

Horses have a well-developed mucosal-associated lymphoid tissue in the naso-oropharynx for immunological defence and the development of immunological tolerance. The different components of this lymphoid tissue have been documented, but not all areas of the equine oral cavity have been investigated. In the present study, samples for histological and immunohistochemical examinations were collected from slaughtered horses of different ages, focusing on the rostral part of the oral cavity. Dense lymphatic tissue was found in the mucosa covering the bar area of the mandibles and the floor of the oral cavity, and it was present in horses of different ages. The most prominent lymphatic tissue, with large aggregates of lymph nodules, was present on either side of the lingual frenulum. The rostral location of this lymphatic tissue in horses renders support for application of antigens in allergen-specific immunotherapy via the oral mucosa.

Keywords: Anatomy, equine, Icelandic horses, immunotherapy, mucosal-associated lymphoid tissue, oral cavity.

YFIRLIT

Hross eru með vel þróaðan slímutengdan eitilvef í nef- og munnkoki þar sem ónæmisvörn og ónæmisþol myndast. Hinum mismunandi þáttum þessa eitilvefs hefur verið lýst en ekki öll svæði munnhols hrossa hafa verið skoðuð. Í þessari rannsókn voru sýni fyrir vefjaskoðun og mótefnalitun tekin úr sláturhrossum á mismunandi aldri, með áherslu á trjónulæga hluta munnholsins. Þéttur eitilvefur fannst í slímhúðinni sem þekur tannlausa bilið í neðri kjálka og í grennd við tunguhaftið. Eitilvefurinn var til staðar í hrossum á ólíkum aldri. Umfangsmesta eitilvefinn, eða safneitlinga, var að finna sitt hvorum megin við tunguhaftið. Staðsetning þessa eitilvefs trjónulægt í munnholinu rennir stoðum undir möguleika þess að hægt sé að þróa ónæmismeðferð um munnslímhúð hrossa.

INTRODUCTION

Mucosal surfaces of the body are endowed with lymphatic tissue for immunological defence and the development of immunological tolerance. An important part of the mucosal immune

system is the mucosal-associated lymphoid tissue (MALT) consisting of tonsils and lymph nodules (Casteleyn et al. 2011, Kumar & Timoney 2005b-d, Kumar & Timoney 2006, Liebler-Tenorio & Pabst 2006). Tonsils, an important component of MALT, are composed of B-cell rich lymphoid follicles and T-cell-dependent interfollicular areas, with close association with the mucosal surface (Liebler-Tenorio & Pabst 2006). MHC-II positive antigen-presenting cells are also an important component of MALT, of which dendritic cells (DCs) are the most efficient cell type (Reinartz et al. 2016). The presence, location, extent, and structure of MALT, including the ring of lymphoid tissue in the naso-oropharynx known as the Waldeyer's ring, varies among different domestic animal species (Casteleyn et al. 2011, Kumar & Timoney 2005b-d, Kumar & Timoney 2006, Liebler-Tenorio & Pabst 2006).

The oral mucosa plays an important role in the development of immunological tolerance. It has been suggested that MALT is biased towards tolerance to antigens due to the extensive exposure to commensal bacteria, food, and environmental material (Reinartz et al. 2016). These qualities make the oral mucosa an attractive site for allergen immunotherapy (AIT) and sublingual immunotherapy (SLIT) is being practiced in humans as an alternative to subcutaneous injections (SCIT) (Dorofeeva et al. 2021, Passalacqua et al 2020). SLIT is currently being developed to treat equine insect bite hypersensitivity (IBH), using transgenic barley and specially designed bits which prolong the time of the barley in the mouth (Jonsdottir et al. 2017). In connection with this research, a pilot study to explore the equine oral cavity was executed, in which an extensive sampling of the oral mucosa of two Icelandic horses was performed (Tryggvason L 2015). The study revealed organized lymphatic tissue present in the mucosa covering the bars of the mandibles and beneath the tongue, in addition to the known tonsillar tissues of the Waldeyer's ring (Casteleyn et al. 2011, Kumar & Timoney 2005b-d, Kumar & Timoney 2006, Liebler-Tenorio & Pabst 2006).

The aim of the present study was to investigate the presence of MALT in the sublingual and bar areas of the mandibles of Icelandic horses of different ages and the cellular components of this lymphatic tissue.

MATERIAL AND METHODS

Heads of two healthy Icelandic horses, a 4-5-year-old colt and a 5-6-month-old foal, were obtained from an abattoir and brought to the Institute at Keldur, where multiple samples from the oral mucosa were collected. Specimens for histology and immunohistochemistry (IHC) were dissected from the floor of the oral cavity beneath the free part of the tongue, including one on either side of, and two rostral to, the frenulum. Four sampling sites were at the gingival-buccal junction along the bars of the mandibles (Figure 1). Two specimens were taken from each location, with one specimen immersed in 10% neutral-buffered formalin and the other in Formalin Free Fixative, Accustain™ (Sigma-Aldrich Co, A542). Procuring Accustain fixed tissue was deemed necessary as antibodies work variably well in formalin-fixed tissue.

Additional material was collected at an abattoir, where tissue samples were dissected from the same areas of the oral cavity from 5 Icelandic slaughtered horses aged from 11 to 22 years. The samples were fixed in 10% neutral-buffered formalin for histology.

Formalin- and Accustain-fixed tissues were trimmed within 5 days after fixation, processed routinely, paraffin embedded, sectioned at 4 mm, mounted on Superfrost microscope slides and stained with haematoxylin-eosin (HE) for histological examination. Cut sections of the formalin- and Accustain-fixed samples from the colt and the foal were also collected on Starfrost slides for IHC (Table 1).

For IHC, sections of formalin- and Accustain-fixed tissue slides were incubated with the primary antibodies at dilutions 1:100 (MHC-II) for one hour at room temperature (RT), and 1:25 (CD3), 1:100 (CD20cy), and 1:25 (CD79a) overnight at 4 ˚C. The slides were then incubated for 30 minutes at RT with the relevant secondary

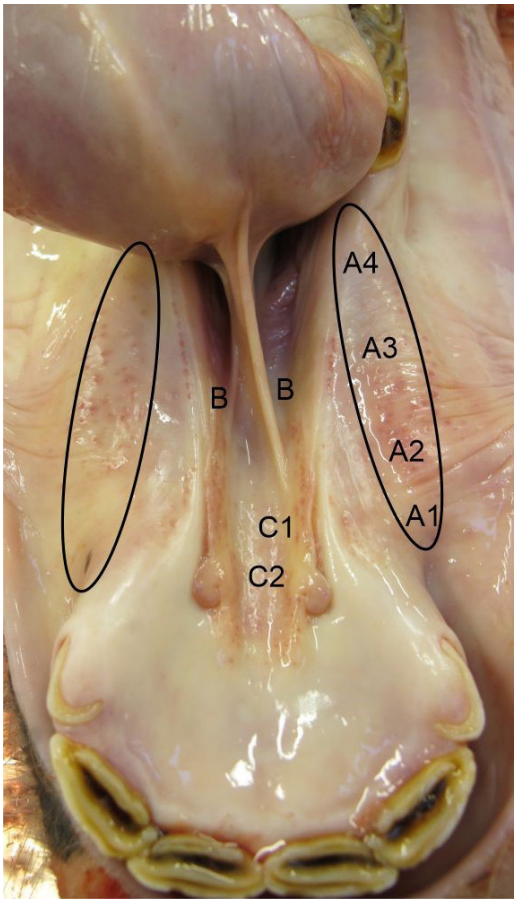

Figure 1. Oral cavity of an Icelandic foal showing areas of tissue sampling.
Four sampling sites along the buccal side of the mandibular bars (A1 – A4). Four samples from the floor of the mouth beneath the free part of the tongue: on either side of the lingual frenulum (B), and rostral to the lingual frenulum (C1 and C2).

antibodies, ready to use Kit K-1500 for MHC-II, and dilutions 1:100 (CD3) and 1:300 (CD20cy and CD79a). Streptavidin HRP (MHC-II), PAP (CD3) or Streptavidin AP (CD20cy and CD79a) was then applied, followed by the substrate solution, DAB (3,3'-diaminobenzidine) or Fast red with Levamisol. After washing, all slides were counterstained with haematoxylin. Formalin-fixed and frozen samples of equine skin, tonsil, and lymph nodes were used as positive controls. For negative controls, slides were incubated with reagent buffer in place of the primary antibody.

RESULTS

Dense lymphatic tissue was present in the lamina propria mucosa in the vicinity of the lingual frenulum and in the bar area of the mandibles of horses aged 6-months-22 years. The lymphatic tissue in the sampled areas consisted of both solitary and variably sized aggregates of lymph nodules (Figures 2a-c). There were also small clusters of loose lymphatic tissue in the superficial lamina propria mucosa, with mainly lymphocytes and the occasional plasma cell.

The lymphatic tissue associated with the tongue was present at the attachment of, and rostrally to, the frenulum (B, C1, C2 in Figure 1, Figure 2b and Figure 3c-e), with the largest aggregates of lymph nodules being on either side of the lingual frenulum (B in Figure 1, Figure 2b and Figure 3c-d). Solitary lymph nodules were the main lymphatic tissue seen in all four sampling sites of the mandibular bar

Table 1. Antibodies and immunohistochemical staining procedures.

Antibody	Clone	Secondary antibody	Detection	Substrate solution
Mouse anti-horse-MHC II[†]	CVS20	Kit K-1500[*] Rabbit & mouse	Streptavidin HRP	DAB[*]
Rabbit anti-human CD3[*]	Polyclonal	Swine Anti-rabbit[*]	Rabbit PAP[¶]	DAB
Mouse anti-human CD20cy[*]	L26	Biotin. rabbit Anti-mouse[*]	Streptavidin AP[§]	Fast Red + Levamisol[¶]
Mouse anti-human CD79a[†]	HM57	Biotin. rabbit Anti-mouse[*]	Streptavidin AP	Fast Red + Levamisol

[†] Bio-Rad Laboratories, Inc Ltd, UK
[*] Dako, Denmark
[¶] Sigma-Aldrich Chemie GmbH, Germany
[§] GE Healthcare UK Limited, UK

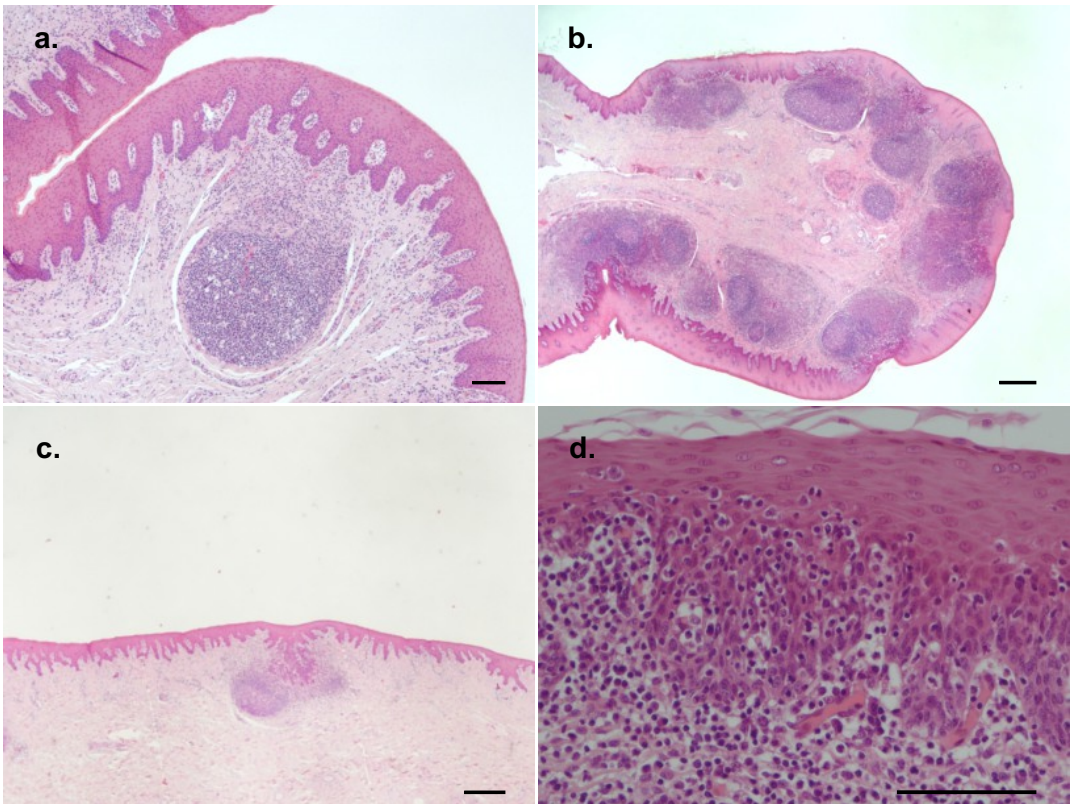

Figure 2. Representative illustration of haematoxylin-eosin-stained sections of formalin-fixed tissue sampled from the oral cavity of Icelandic horses.

a. Solitary lymph nodule in the lamina propria mucosa of the mandibular bar area; 4-5-year-old colt.
b. Aggregates of lymph nodules in the lamina propria mucosa, lateral to the lingual frenulum; 18-year-old horse.
c. Solitary lymph nodule in the lamina propria mucosa of the mandibular bar area. Irregular pegs from the mucosal epithelial lining extend down to the lymphatic tissue; 21-year-old horse.
d. The mucosal epithelial lining lateral to the lingual frenulum has irregular pegs with indistinct borders due to numerous infiltrating leukocytes; 5-6-month-old foal.

Bar = 100 mm

area (A1-4 in Figure 1, Figure 2a and c, and Figure 3a and b).

The oral cavity in these regions was lined by a non-keratinized squamous epithelium with short, plump, somewhat irregular pegs extending into the lamina propria mucosa. In areas, the epithelium was slightly indented, sometimes attenuated, and indistinct because of infiltrating leukocytes (Figures 2d and 3f), but no follicular crypts or M-cells were seen.

For the antibodies detecting MHC-II, CD3, CD20cy and CD79a, the results of IHC for formalin- and Accustain fixed samples were comparable. CD20cy and CD79a positive B-cells were the predominant cell type in the lymph nodules, with CD3 positive T-cells at the outer borders (Figures 3a-d). A mixture of B- and T-lymphocytes were in the internodular areas of aggregated lymph nodules and in the adjacent diffuse lymphatic tissue (Figure 3a-d). Many of the cells in the dense and adjacent diffuse lymphatic tissue expressed MHC-II, as well as cells around blood vessels just beneath the mucosal epithelial lining (Figure 3e). Cells

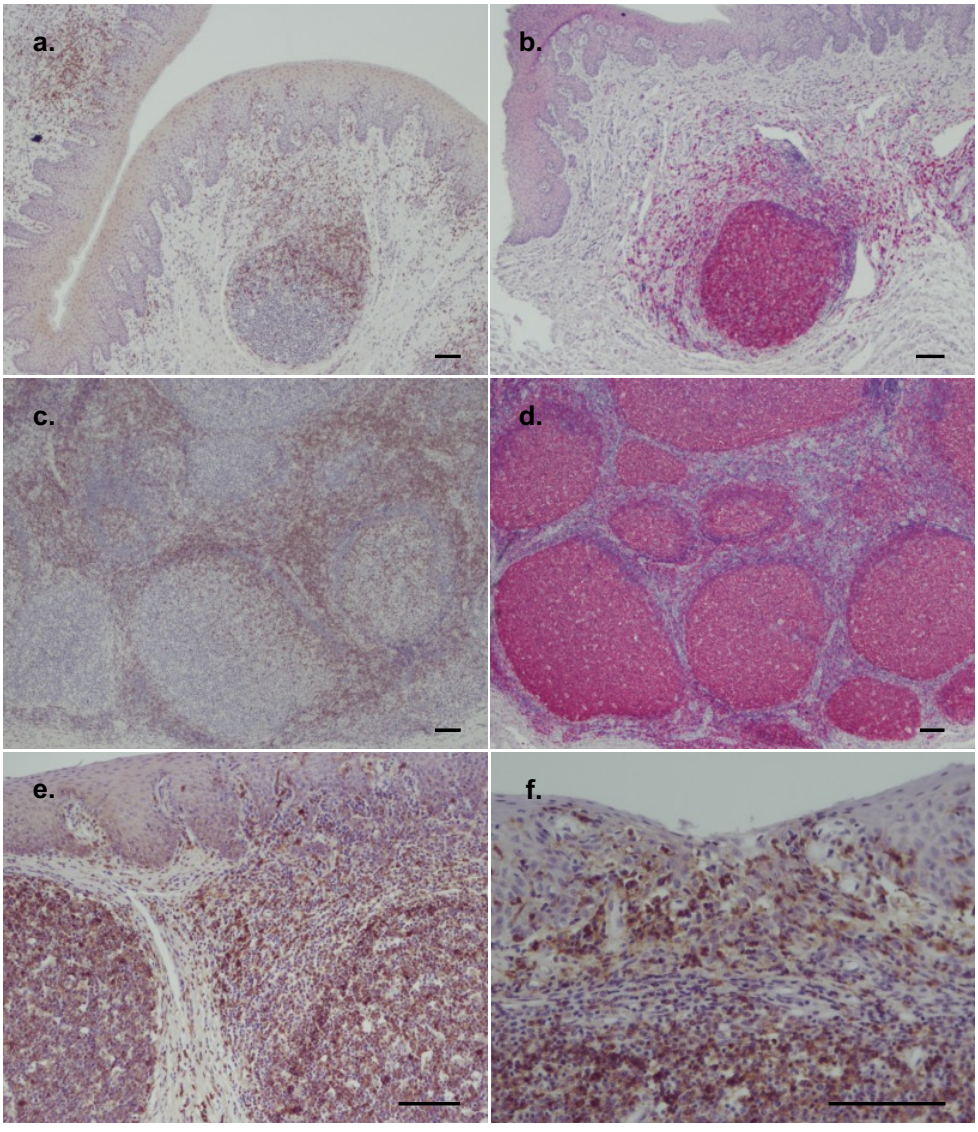

Figure 3. Representative illustration of immunohistochemical stained sections of fixed tissue sampled from the oral cavity of Icelandic horses.

a. CD3 positive T-lymphocyte form a cap towards the oral cavity on a solitary lymph nodule in the mandibular bar area, same location as in figure 2a; 4-5-year-old colt.
b. CD20yc positive B-cells are the predominant cell type in a solitary lymph nodule in the mandibular bar area and B-cells are also present in the loose lymphatic tissue surrounding the nodule; 5-6-month-old foal.
c. Aggreagates of lymph nodules lateral to the lingual frenulum. CD3 positive T- lymphocytes are at the outer borders and between the lymph nodules; 5-6-month-old foal.
d. Same area as in figure 3c with CD20yc positive B-cells prevailing in the lymph nodules.
e. Numerous MHC-II positive leukocytes in two lymph nodules and in the loose lymphatic tissue beneath the mucosal epithelium, lateral to the lingual frenulum; 4-5-year-old colt.
f. Attenuated, irregular mucosal epithelial lining in the mandibular bar area, with blurred outlines due to infiltrating MHC-II positive leukocytes; 5-6-month-old foal.

Formalin-fixed samples; figures a-d. Accustain-fixed samples; figures e and f. Bar = 100 mm

infiltrating the mucosal epithelium were MHC-II (Figure 3f) and CD3 positive, with fewer CD20cy and CD79a positive cells.

DISCUSSION

The present study verified the presence of dense lymphatic tissue in the oral mucosa beneath the tongue and in the bar area of the mandibles in Icelandic horses. Histological and immunohistochemical composition of this lymphatic tissue fulfils the criteria of MALT in general and non-cryptic tonsils in particular, corresponding to tonsillar tissue in other parts of the oral cavity (Liebler-Tenorio & Pabst 2006, Casteleyn et al 2011, Kumar & Timoney 2005b). Lymphatic tissue at these two locations of the rostral oral cavity persists into adult life and does not involute like the ileal Peyer's patches (IPP), as it was present in horses age under 1 year and up to 22 years. This study did not, however, ascertain whether this lymphatic tissue was constitutively present or whether, like the bronchial associated lymphoid tissue (BALT) in horses, it develops after antigen encounter (Liebler-Tenorio & Pabst R 2006). The mucosal lining, with its infiltrating leukocytes, also parallels the description of the follicular associated epithelium (FAE) of other tonsillar tissues (Liebler-Tenorio & Pabst 2006, Kumar & Timoney 2005a).

MHC-II positive cells were present in this lymphatic tissue and in the mucosal epithelium, but the present study could not verify whether they represented professional antigen-presenting cells. Several specific antibodies for antigen-presenting cells were tested on formalin and Accustain-fixed tissue, in addition to frozen tissue sampled from the foal and the colt, without positive results.

This paper describes MALT in the rostral oral cavity of Icelandic horses that should make allergen-specific immunotherapy via the oral mucosa feasible (Jonsdottir S 2017).

REFERENCES

Casteleyn C, Breugelmans S, Simoens P & Van den Broeck W 2011. The tonsils revisited: Review of the anatomical localization and histological characteristics of the tonsils of domestic and laboratory animals. *Clin Dev Immunol*. https://doi.10.1155/2011/472460.

Dorofeeva Y, Shilovskiy I, Tulaeva I, Focke-Tejkl M, Flicker S, Kudlay D, Khaitov M, Karsonova A, Riabova K, Karaulov A, Khanferyan R, Pickl W-F, Wekerle T & Valenta R 2021. Past, present, and future of allergen immunotherapy vaccines. *Allergy* 76, 131-149. https://doi.10.1111/all.14300.

Jonsdottir S, Svansson V, Stefansdottir S-B, Mäntylä E, Marti E & Torsteinsdottir S 2017. Oral administration of transgenic barley expressing a Culicoides allergen induces specific antibody response. *Equine Vet J* 49, 512-518. https://doi.10.1111/evj.12655.

Kumar P & Timoney J-F 2005a. Histology and ultrastructure of the equine lingual tonsil. I. Crypt epithelium and associated structures. *Anat Histol Embryol* 34, 27-33. https://doi.10.1111/j.1439-0264.2004.00560.x.

Kumar P & Timoney J-F 2005b. Histology and ultrastructure of the equine lingual tonsil. II. Lymphoid tissue and associated high endothelial venules. *Anat Histol Embryol* 34, 98-104. https://doi.10.1111/j.1439-0264.2004.00579.x.

Kumar P & Timoney J-F 2005c. Histology, immunohistochemistry and ultrastructure of the equine tubal tonsil. *Anat Histol Embryol* 34,141-148. https://doi.10.1111/j.1439-0264.2005.00582.x.

Kumar P & Timoney J-F 2005d. Histology, immunohistochemistry and ultrastructure of the equine palatine tonsil. *Anat Histol Embryol* 34, 192-198. https://doi.10.1111/j.1439-0264.2005.00594.x.

Kumar P & Timoney J-F 2006. Histology, immunohistochemistry and ultrastructure of the tonsil of the soft palate of the horse. *Anat Histol Embryol* 35, 1-6. https://doi.10.1111/j.1439-0264.2005.00622.x.

Liebler-Tenorio E-M & Pabst R 2006. MALT structure and function in farm animals. *Vet Res* 37, 257-280. https://doi.10.1051/vetres:2006001.

Passalacqua G, Bagnasco D, Canonica G-W 2020. 30 years of sublingual immunotherapy. *Allergy* 75, 1107-1120. https://doi.10.1111/all.14113.

Reinarz S-M, van Tongeren J, van Egmond D, de Groot E-J-J, Fokkens W-J & van Drunen C-M 2016. Dendritic cell subsets in oral mucosa of allergic and healthy subjects. *Plos One* 11. https://doi.10.1371/journal.one.0154409.

Tryggvason L 2015. Distribution and Characteristic of Lymphoid Tissue within the Equine oral mucosa. BVetMed Thesis (EMS No:S364). Royal Veterinary College, University of London, UK

Received: 15.12.2023
Accepted: 12.3.2024

www.ias.is
https://doi.org/10.16886/IAS.2024.02 ICEL. AGRIC. SCI. 37 (2024), 11-24

Tree-ring width and stable isotope analyses of *Picea sitchensis* from Iceland reveal growth potential under predicted climate change

Petr Čermák[1], Tomáš Kolář[2, 3], Michal Rybníček[2, 3], Tomáš Žid[1], Otmar Urban[3], Natálie Pernicová[3, 4], Ólafur Eggertsson[5, 9], Eva Koňasová[2], Ulf Büntgen[3, 6, 7, 8]

[1] Department of Forest Protection and Wildlife Management, Faculty of Forestry and Wood Technology, Mendel University in Brno, Czech Republic

[2] Department of Wood Science and Technology, Faculty of Forestry and Wood Technology, Mendel University in Brno, Czech Republic

[3] Global Change Research Institute of the Czech Academy of Sciences (CzechGlobe), Brno, Czech Republic

[4] Department of Agrosystems and Bioclimatology, Faculty of AgriSciences, Mendel University in Brno, Czech Republic

[5] Land and Forest Iceland, Reykjavik, Iceland

[6] Department of Geography, Faculty of Science, Masaryk University, Brno, Czech Republic

[7] Department of Geography, University of Cambridge, UK

[8] Swiss Federal Research Institute (WSL), Birmensdorf, Switzerland

[9] Agricultural University of Iceland, Hvanneyri, Iceland

ABSTRACT

Sitka spruce has been one of the most planted tree species in Iceland since the mid-twentieth century. Here, we use different dendrochronological methods to identify the controlling climatic factors of its growth and possible changes in their influence over time. We develop annually resolved and absolutely dated measurements of tree-ring width (TRW) from 21 trees and oxygen ($\delta^{18}O$) and carbon ($\delta^{13}C$) stable isotopes from six trees to evaluate growth trends and climate sensitivity in Iceland's Hallormsstaður National Forest over the past 54 years (1965–2018). Warmer and wetter summers in the last few decades have resulted in significantly increasing radial growth. While TRW and $\delta^{13}C$ reflect strong July-August temperature signals, with the highest correlation for July, $\delta^{18}O$ is mainly controlled by the temperature in March. The occurrence of negative pointer years in TRW decreases with increasing temperature in July but increases with excessive precipitation in August. Our study shows great continued potential for Sitka spruce cultivation in Iceland.

Keywords: afforestation, climate change, precipitation, dendrochronology, temperature

YFIRLIT

Mælingar á árhringjabreiddum og stöðugra samsætna í sitkagrein frá Íslandi sýna vaxtargetu við spár um loftslagsbreytingar.

Frá miðri tuttugustu öldinni hefur sitkagreni verið ein af mest gróðursettu trjátegundum á Íslandi. Við notuðum aðferðir árhringjarannsókna til að greina þá umhverfisþætti sem hafa mestu áhrif á vöxt og viðgang sitkagrenis á Hallormsstað og þær breytingar sem hafa orðið á áhrifum umhverfisþátta gegnum árinn. Við byggðum upp tímatal fyrir árhringjavöxtinn með því að mæla breiddir árhringjanna í 21 tré, þannig að hver árhringur fékk sitt ártal og meðalbreidd. Einnig mældum við stöðugar samsætur súrefnis ($\delta^{18}O$) og kolefnis ($\delta^{13}C$) í árhringjum

sex trjáa. Þetta var framkvæmt til þess að meta árlegan vöxt og áhrif veðurfars á viðgang trjánna/skógarins. Sýnum var safnað í Hallormsstaðarskógi og nært árhringjatímatalið aftur til ársins 1965 eða síðustu 54 árin (1965–2018). Hlýr og rök sumur á síðustu áratuga hafa leitt til verulegs aukins þvermálsvaxtar í sitkagreninu. Á meðan árhringjavöxtur og $\delta^{13}C$ endurspeglar góða fylgni við sumarhita í júlí–ágúst og hæstu fylgni fyrir júlí hita er $\delta^{18}O$ aðallega stjórnað af hitastigi í mars. Tíðni neikvæðs árhringjavaxtar minnkar með hækkandi hitastigi í júlí en eykst ef águstmánuður er úrkomusamur. Rannsókn okkar sýnir að framtíðarhorfur ræktunar sitkagrenis eru góðar á Íslandi þrátt fyrir væntanlegar breytingar á veðurfari.

INTRODUCTION

Sitka spruce (*Picea sitchensis*) is one of the most important species used for afforestation in Iceland, accounting for 14 % of all trees planted from 1940 to 1998 (Sigurdsson & Snorrason 2000). Afforestation by planting trees, especially exotic spruces, pines and larches, was very intensive in the 1950s and the first half of the 1960s (Blöndal & Gunnarsson 1999, as cited in Reynisson 2011). Planting declined after 1963 when extreme spring frost damaged a large proportion of planted forests in southern and western Iceland. The afforestation programme was restarted at the end of the 20th century (Eggertsson et al. 2008) to increase carbon sequestration in forests, vegetation and soil (Sigurdsson & Snorrason 2000). Sitka spruce plays a key role in afforestation, as it makes up the largest growing stock of any exotic planted tree species (Snorrason et al. 2005).

In June 2020, the Icelandic government published an updated Climate Action Plan (Government of Iceland 2020), an important aim of which was to increase carbon sequestration through improved land use, land use change and forestry. Changing climate conditions can markedly influence the growth and vitality of cultivated forests and consequently amount of carbon sequestration. Therefore, a better understanding of the climate-growth relationship is fundamental for forest carbon stock prediction. It may contribute to improved decision-making about the potential of Sitka spruce for commercial timber production, as well as for carbon sequestration under current and projected Icelandic climatic conditions.

Several tree-ring studies of Sitka spruce have been carried out within the natural distribution of Sitka spruce in North America (Wiles et al. 1998, Barclay et al. 1999), as well as outside its natural distribution, where Sitka has been planted because of its fast growth and relative resistance, e.g., Norway, Iceland, Scotland, Denmark, Poland and Estonia (Feliksik & Wilczyński 2008 & 2009, Vihermaa 2010, Huang 2017, Läänelaid & Helama 2019, Kasesalu et al. 2019, Kuckuk et al. 2021). However, in these studies climate sensitivity was assessed using conventional tree-ring width. Missing from these studies was the exploitation of other tree-ring parameters more sensitive to environmental factors that allow a better understanding of climate change impacts, processes of physiological acclimation, and succession.

Dendrochronological analyses have been carried out in Iceland to examine the effects of climate change on various native species, both trees and shrubs (e.g., Levanič & Eggertsson 2008, Piermattei et al. 2017, Hannak & Eggertsson 2020, Phulara et al. 2022, Frigo et al. 2023, Opała-Owczarek et al. 2024). Our study complements the results of these analyses with findings from non-native *Picea sitchensis.*

We selected one of the oldest forest stands in Iceland, planted in the 1960s, to retrospectively evaluate its radial growth and climate sensitivity in relation to its potential for future planting in sub-Arctic regions. The main aims of our research were i) to evaluate the growth trends of Sitka spruce over the last ~60 years, and ii) to explore its climate sensitivity and limitations using tree-ring width and stable carbon and oxygen isotope ratios of non-pooled, annually resolved tree rings. Our hypotheses were: i) Sitka spruce growth is mainly influenced by the temperature in the growing season; precipitation

does not have a significant effect on growth due to relatively high amounts of precipitation; ii) anthropogenic climate change has already led to enhanced radial growth. A better understanding of growth trends and the climate factors driving them can contribute to assessing the potential of Sitka spruce in Iceland, both from an environmental (carbon sequestration) and timber production perspective.

MATERIALS AND METHODS

Study area and climatic data

The *Picea sitchensis* sampling site is located in Hallormsstaður National Forest in East Iceland (Figure 1, Table 1). The forest covers an area of 740 hectares, most of which is dominated by native birch, but there are also cultivated forests of various species and experimental forests. In June 2019, we selected 21 representative dominant trees in the forest stand and measured their height and circumference at breast height (1.3 m above ground level). As a measure of tree crown condition, we further evaluated two basic parameters visually (Cudlín et al. 2001) – total defoliation (%) and discoloration, i.e., yellowing and browning (as a % of the total volume of a crown with discoloration). We evaluated the parameters at intervals of 5 % based on the scale defined by Cudlín et al. (2001) (Table 1).

Table 1. Hallormsstaður sampling site – stand information and mean climatic conditions

Latitude/Longitude	N 65°06'10.5"	W 14°43'42.2"
TREE PARAMETERS	Min.-Max.	Mean
Tree height	18.4–23.6 m	20.8 m
Circumference at breast height	92–156 cm	120.3 cm
Defoliation	5–25 %	11.7 %
Discoloration	absent	absent
CLIMATE CONDITIONS 1965–2018*	Min.-Max.	Mean
Annual temperature	1.5–5.2 °C	3.6 °C
May-August temperature	7.0–10.4 °C	8.8 °C
Annual precipitation	332–1,669 mm	833 mm
May-August precipitation	51–340 mm	169 mm

** determined on the basis of data compiled from three meteorological stations*

Climate data from three meteorological stations were available and relevant for the study area (Figure 1). The Hallormsstaður station data are discontinuous for temperature (1965–1989 and 1997–2018) and precipitation (1965–1989

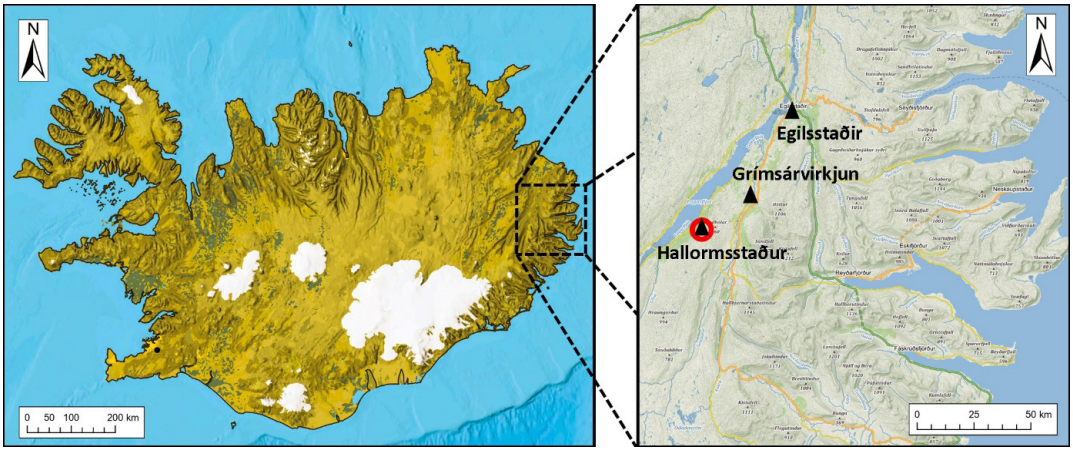

Figure 1. Location of the study site (red circle) and meteorological stations (black triangles). Coordinates of climate stations: Grímsárvirkjun – N 65°08'15.1" W 14°31'56.4"; Hallormsstaður – N 65°05'39" W 14°43'1"; Egilsstaðir – N 65°16'12" W 14°23'32".

and 2002–2018). The Egilsstaðir station data were available only for temperature and cover the whole study period (1965–2018). The Grímsárvirkjun station data were recorded only for precipitation from 1965 to 2013. Since none of the stations provided temperature and precipitation measurements covering the whole study period (1965–2018), we averaged data from the stations into one series for each climate parameter. To verify the average temperature and precipitation data, we compared the averaged station series with climate data from the Climate Research Unit – CRU database (CRU TS4.04; via http://climexp.knmi.nl), which are frequently used in dendroclimatological studies. The comparison shows that CRU data underestimated temperatures and overestimated precipitation, as might be expected in the conditions of Iceland, which are characterised by great spatial variability of climatic parameters (especially precipitation). However, the climate data from both resources are highly correlated (Figure 2). Based on these findings, we decided to use averaged data from meteorological stations for the further analysis.

The climate conditions are characterised by high variability in annual precipitation (with a minimum of 332 mm in 1965 and a maximum of 1,669 mm in 2002), with highest rainfall in November and December (a total of 736 mm in these two months). The annual mean temperature was lowest in 1979 (1.5 °C) and highest in 2014 (5.2 °C). Monthly mean temperatures from December to March were below 0 °C. The warmest months were July and August with mean temperatures slightly above 10 °C.

Tree-ring width and stable isotope measurement

We extracted one core per tree at breast height (Kirdyanov et al. 2018) from all 21 selected trees, using a Pressler borer (Haglöf Company Group, Sweden) with a 5-mm inner diameter. Tree-ring width was measured on the cores, using a VIAS TimeTable device with a measurement length of 78 cm (SCIEM, Vienna, Austria). The obtained TRW series were cross-dated and corrected for missing and false rings, using both PAST4 (Knibbe 2004) and COFECHA (Grissino-Mayer 2001, Holmes 1983).

Then, six randomly selected and absolutely dated Sitka spruce core samples were separated with annual resolution. We selected this sample size to maintain sufficient climate signal strength for the isotopic chronologies and in recognition of the financial expense of isotope analysis (Rybníček et al. 2021). Each tree ring was cut into small pieces with a razor blade under a stereomicroscope and packed into F57 Teflon filter bags (Ankom Technology, USA) for alpha-cellulose extraction according to the modified Jayme-Wise isolation method as described in Urban et al. (2021).

The homogenised samples of alpha-cellulose (0.8–1.0 mg) were weighed into tin and silver capsules to determine carbon and oxygen isotopes, respectively. For the $\delta^{13}C$, the alpha-cellulose was combusted to CO_2 at 960 °C, while it was pyrolysed to CO at 1,450 °C for $\delta^{18}O$ measurement using a vario PYRO cube elemental analyser (Elementar Analysensysteme, Germany). The ratios between heavy (^{13}C and ^{18}O) and light (^{12}C and ^{16}O) stable isotopes were determined using an IsoPrime100 continuous flow mass spectrometer (Isoprime, UK). The spectrometer was internally calibrated using certified analytical standards with known isotopic ratios: caffeine (IAEA-600) and graphite (USGS24) for $\delta^{13}C$ and benzoic acids (IAEA-601 and IAEA-602) for $\delta^{18}O$. The $\delta^{13}C$ and $\delta^{18}O$ values (‰) are expressed relative to the Vienna Pee Dee Belemnite (VPDB) and Vienna Standard Mean Ocean Water (VSMOW) standards, respectively. In addition, the $\delta^{13}C$ series were corrected for atmospheric ^{13}C depletion due to fossil fuel burning using a ^{13}C Suess correction model based on Mauna Loa atmospheric CO_2 concentrations (Dombrosky 2020). For further details see Urban et al. (2021) and Römer et al. (2023).

Growth trends of the raw TRW, $\delta^{13}C$ and $\delta^{18}O$ chronologies, as well as the trends of the climatic parameters used (temperature and precipitation), were assessed over the study period (1965–2018), and their statistical

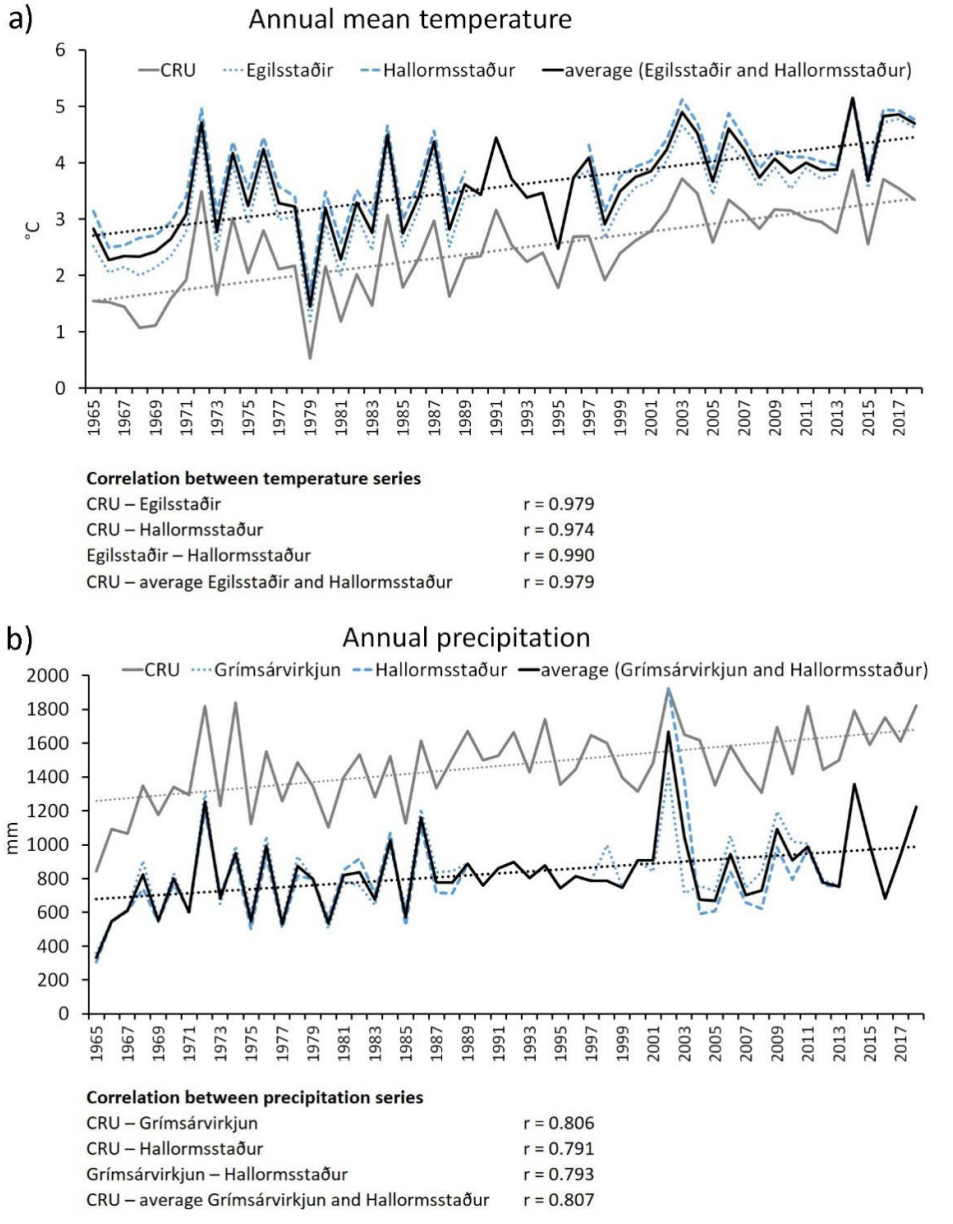

Figure 2. Comparison of CRU climate data and meteorological station data: a) annual mean air temperature with linear trend; b) annual precipitation with linear trend.

significance was determined using the Mann-Kendall test. Pettitt's test (Pettitt 1979) was applied to detect a single change-point in the chronologies, as well as in the meteorological series.

Non-climatic, size- and age-related growth trends and other factors were removed from the individual series by applying four different detrending techniques in Arstan (Cook & Krusic, 2005): cubic smoothing splines with

a 50 % frequency response cutoff at 32 and 50 years (spline32, spline50), negative exponential function (neg exp) and regional curve standardisation (rcs). All methods were used to preserve high frequency (inter-annual) variations for climate-growth analysis (Cook & Peters 1981). All indices were calculated as residuals after the adaptive power transformation of the raw data to minimise end-effect problems (Cook & Peters 1997). Chronologies were calculated using bi-weight robust means. Internal signal strength was assessed using inter-series correlation (Rbar) and the expressed population signal (EPS; Wigley et al. 1984). All indexed chronologies, displaying small differences among each other (Figure 3), were used for correlations with climate data (Figure 4).

Since detrending climate data can better capture tree growth sensitivity to climate (Ols et al. 2023), we detrended temperature and precipitation series using the same method as the TRW series. We calculated correlation coefficients between the indexed chronologies and climatic parameters in the period 1965–2018. Monthly values of climatic parameters from January to August of the year of tree-ring formation were considered. The correlations were calculated for monthly values, as well as seasonal means for January-August (the whole year), May-August (vegetation period), and July-August (summer months with expected highest effect). As the best correlation results were obtained using cubic smoothing splines with a 50 % frequency response cutoff at 32 years (Figure 4a, 5), the spline32 chronology was used for further analyses. For the periods with the strongest significant correlations, we performed 19-year moving correlations (window ±9 years) to test the stability of these relationships (Figure 4b).

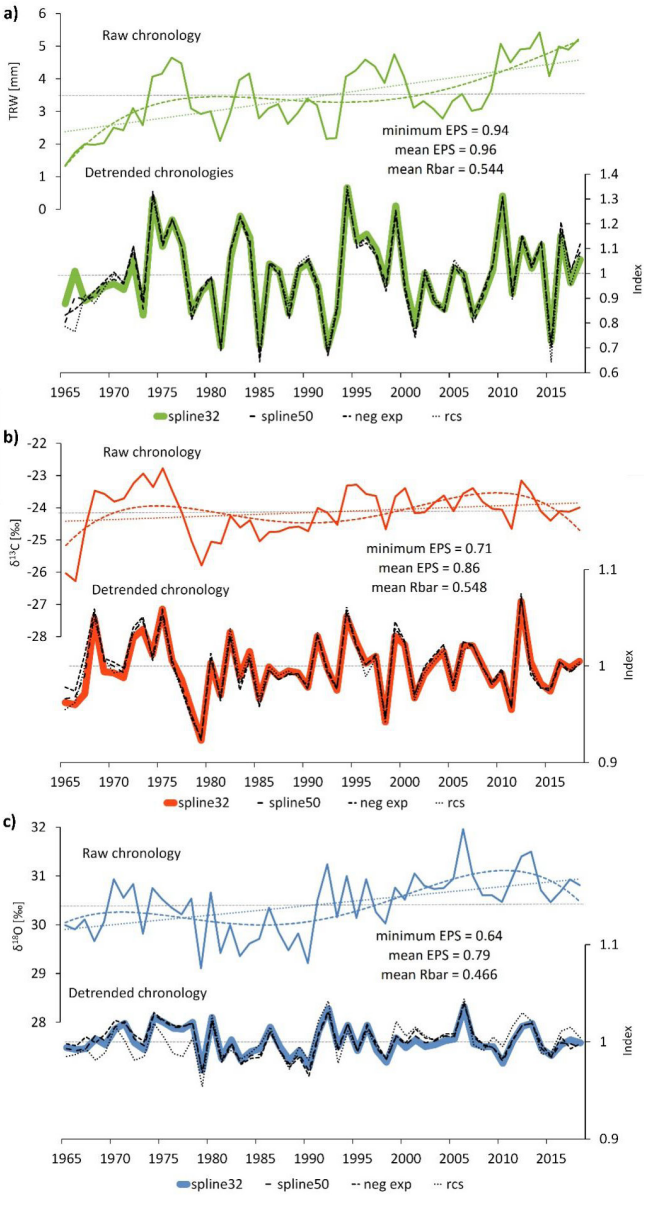

Figure 3. Raw and detrended chronologies (spline32, spline50, neg exp, rcs) of tree-ring width **(a)**, $\delta^{13}C$ **(b)** and $\delta^{18}O$ **(c).** Dashed lines in the raw chronologies are polynomial trend lines, dotted lines are linear trend lines.

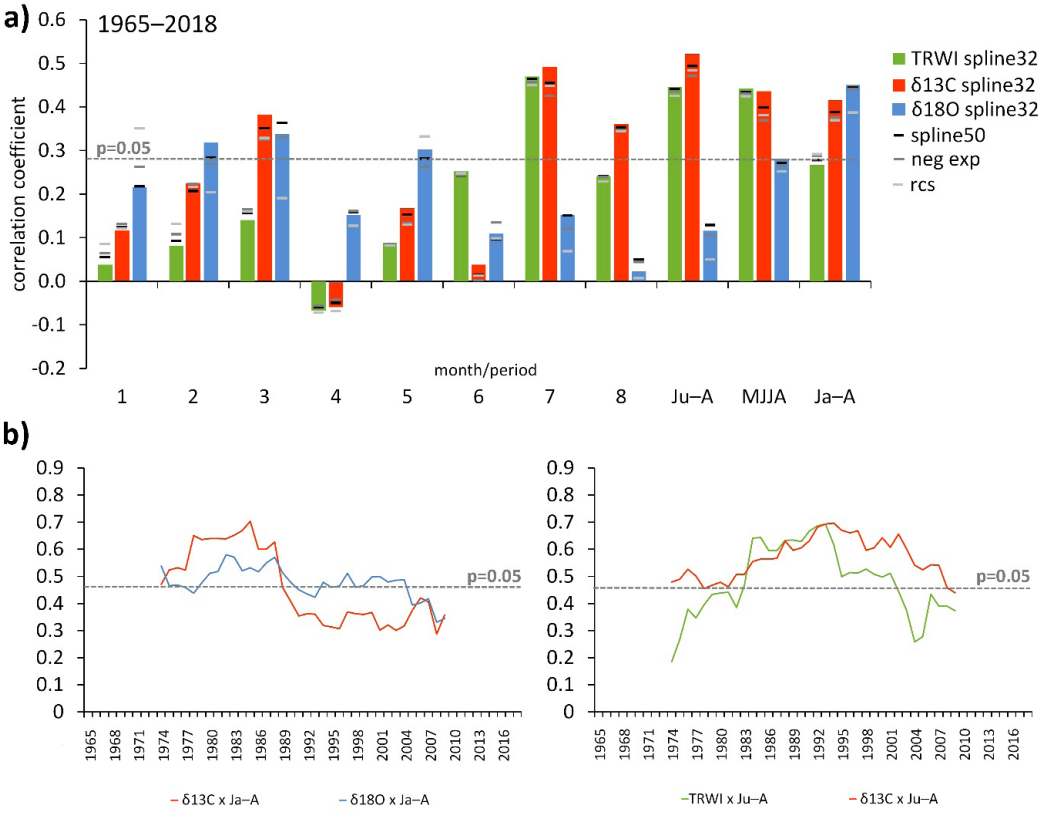

Figure 4. a) Pearson's correlation coefficients between temperature and residual TRW, $\delta^{13}C$ and $\delta^{18}O$ chronologies from 1965 to 2018; **b)** 19-year moving correlation between January-August (Ja-A) temperature and $\delta^{13}C$ (red line) and $\delta^{18}O$ (blue line) and for July-August (Ju-A) temperature and TRWI (green line) and $\delta^{13}C$ (red line).

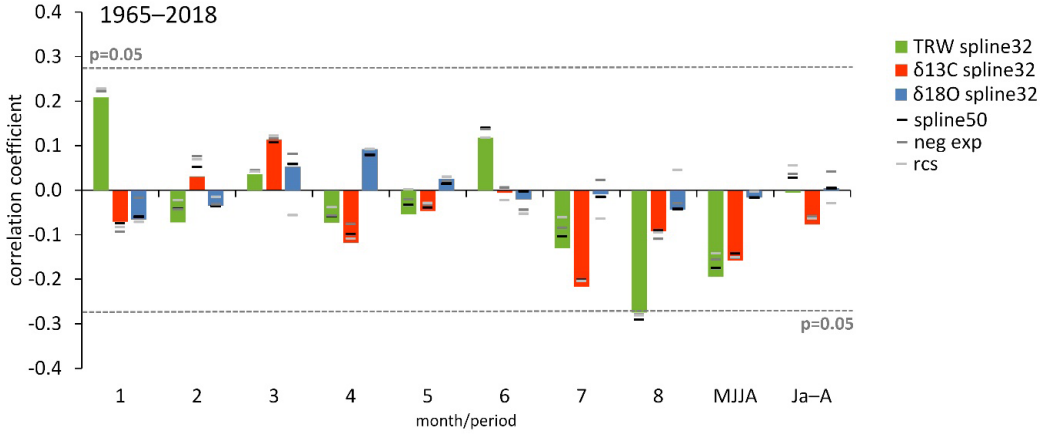

Figure 5. Pearson's correlation coefficients between precipitation and residual TRW, $\delta^{13}C$ and $\delta^{18}O$ chronologies from 1965 to 2018.

Furthermore, negative and positive extremes of tree-ring width chronology were correlated with the climate parameters to determine their influence on the significantly reduced or enhanced radial growth of Sitka spruce trees. The negative/positive extremes were determined for years in which residual TRWI chronology exceeded the ±1.0 multiple of a standard deviation subtracted/added to the mean (Jetschke et al. 2019). The threshold value was arbitrarily defined to yield a sufficient number of extreme years. The relationships between the negative/positive extremes and climate parameters were evaluated using a logistic regression (Quinn & Keough 2002), for which the binary response was coded as a "normal" year (Value 0) or a negative/positive extreme year (Value 1). Models were verified at the first step using Wald's test for regression parameters and goodness of fit (Quinn & Keough 2002). At the second step, only significant models were tested using the likelihood ratio test. The model was considered of merit if both of these tests reached the 0.05 significance level.

RESULTS

Data characteristics

The chronologies covering the period 1965−2018 were replicated by 21 trees for TRW and by six trees for stable carbon and oxygen isotopes. The lowest first-order autocorrelation was observed for the $\delta^{18}O$ chronology (0.246), while for the $\delta^{13}C$ (0.556) and TRW chronologies it was more than double (0.683), which indicated much greater temporal memory. The highest year-to-year variability, expressed as the mean sensitivity, was observed for TRW (0.228), whereas the values for carbon and oxygen stable isotopes were close to zero (0.036 and 0.028, respectively).

The average tree-ring width varied between 1.34 (1965) mm and 5.43 mm (2014). TRW had a statistically significant increasing growth trend (Mann-Kednall test, $S = 681$, $p < 0.001$), especially in the last ten years (Figure 3a). Based on Pettitt's test, the significant change point of the linear trend occurred in 1993 ($p < 0.00005$).

The mean carbon and oxygen isotope values were -24.13‰ ($\delta^{13}C$) and 30.42‰ ($\delta^{13}O$), respectively. The standard deviations were 0.74 for $\delta^{13}C$ and 0.60 for $\delta^{13}O$. During the study period 1965–2018, stable isotopic chronologies also demonstrated an increasing linear trend (Figure 3b, c), statistically significant for $\delta^{18}O$ (Mann-Kednall test, $S = 484$, $p < 0.0004$) but not significant for $\delta^{13}C$ (Mann-Kednall test, $S = 191$, $p = 0.1563$).

The statistically significant increasing positive trend was also observed for both mean annual temperatures (Mann-Kednall test, $S = 694$, $p < 0.001$) and for annual precipitation totals (Mann-Kednall test, $S = 394$, $p < 0.01$) (Figure 2). Pettitt's test revealed the significant change point of the linear trend only for annual mean temperature in 1999 ($p < 0.001$).

Climate sensitivity

We correlated the detrended climate data with the residual TRW, $\delta^{13}C$ and $\delta^{18}O$ chronologies. TRW and $\delta^{13}C$ reflected mainly a positive temperature signal, especially in summer (Figure 4a). The strongest correlations for both TRW and $\delta^{13}C$ were identified for July ($r=0.470$ and 0.492, respectively) and July-August ($r=0.446$ and 0.522, respectively). $\delta^{18}O$ is mainly controlled by temperature in the winter and spring months (mostly March with $r=0.337$); however, the strongest correlations were identified for January-August temperature ($r=0.450$).

We made 19-year moving correlations for the period with the strongest correlations (Figure 4b), to assess their temporal variability within a relatively short chronology. The relationship between the July-August temperature and TRWI was statistically significant only during the 1980s and the 1990s, otherwise the correlations were slightly below the significance level. The relationship between the July-August temperature and $\delta^{13}C$ was stable and significant for the whole period. The relationship between the January-August temperature and $\delta^{13}C$ was above the significance level until the late 1980s, when it dropped and ranged between 0.3 and 0.4. The relationship between the January-August

Table 2. Logistic regression results – relationships between negative pointer years and climatic parameters

Extremes	Climatic parameter	Estimate	Std. error	z value	p (>|z|)	Likelihood ratio test
Negative	Temperature (July)	-0.8069	3.1664	-2.535	0.0395	0.005
	Precipitation (August)	0.0341	0.0127	2.677	0.0074	0.003

temperature and $\delta^{18}O$ was also relatively stable for the whole period; the correlation coefficient values were around the significance threshold.

Precipitation does not play an important role for Sitka spruce growth. None of the three tree-ring parameters showed any significant correlations (Figure 5) except for a relationship between TRWI and August precipitation (r=-0.275).

To assess abrupt growth changes in TRW, positive and negative pointer years were calculated. We identified eight negative pointer years (1965, 1981, 1985, 1988, 1992, 2001, 2007, 2015) and seven positive pointer years (1974, 1976, 1983, 1994, 1999, 2010, 2016). We found two statistically significant relationships between negative pointer years and climatic parameters. The probability of a negative pointer year occurrence decreased with increasing temperature in July and increased with increasing precipitation in August (Table 2). We found no relationship between positive pointer years and climatic parameters.

DISCUSSION

Climatic signals

The natural occurrence of *Picea sitchensis* is associated with hypermaritime to maritime cool mesothermal climate conditions (Klinka et al. 1990), i.e., areas with high annual precipitation and cool moist summers (Franklin et al. 1972, Griffith 1992). The best sites for Sitka spruce have deep, moist, well-drained soils. Hallormsstaður is a cold site with high annual precipitation (Table 1, Figure 2), i.e., it has good conditions for the growth of Sitka spruce. Tree-ring width has an increasing trend, especially in the last ten years (Figure 3a). We found significant positive correlations of tree-ring parameters with temperature in the growing season and the absence of significant correlations with precipitation. The positive effect of summer temperatures on radial growth is confirmed by the observed decreasing probability of a negative pointer year occurrence with increasing July temperature (Table 2). Our findings are consistent with other studies from northern regions, especially from Alaska, where summer temperatures have been identified as a major driver of tree ring development of Sitka spruce, and where precipitation plays only a minor role (Wiles et al. 1998, Barclay et al. 1999). Summer temperatures have been identified as a major factor positively controlling tree-ring width even for plantings in the Southern Hemisphere, specifically on subantarctic Campbell Island (Palmer et al. 2017). However, in areas with higher average temperatures (Poland, Estonia, Scotland, Denmark), temperature often had no effect on tree-ring width (Vihermaa 2010, Huang 2017) or had only negative effect (Vihermaa 2010). If a positive effect was identified for this areas, it was found only for winter and early spring (Feliksik & Wilczyński 2008 & 2009, Läänelaid & Helama 2019). On the contrary, the effect of precipitation on tree-ring width has occurred at the expense of temperature, and in particular, the positive effect of precipitation in the summer months (Feliksik & Wilczyński 2008 & 2009, Vihermaa 2010, Huang 2017, Läänelaid & Helama 2019).

We found increasing trends in $\delta^{13}C$ and $\delta^{18}O$ values and in their significant positive correlations with temperature during the growing season. Values of $\delta^{13}C$ depend on factors influencing the photosynthetic uptake of CO_2 and are primarily controlled by stomatal conductance and the rate of carboxylation during photosynthesis (Farquhar et al. 1989). On the contrary, $\delta^{18}O$ values are closely related

to the isotopic composition of the source water and the rate of H_2O transpiration (Barbour & Farquhar 2004). Enhanced transpiration, a process stimulated by high temperature and low relative air humidity, leads to the enrichment of ^{18}O in leaves and subsequently its higher representation in synthesised carbohydrates and cellulose (Porter et al. 2009, Esper et al. 2018). Accordingly, the climatic signal of $\delta^{18}O$ decreases in the cold and wet environments of arctic regions.

It is well known that stomata close under water-limited conditions. The consequent low conductance for CO_2 diffusion through stomata reduces ^{13}C discrimination in plants and leads to changes in $\delta^{13}C$ (Gagen et al. 2004, Porter et al. 2009). In humid conditions, however, the key factors influencing $\delta^{13}C$ are solar radiation and temperature, modulating the photosynthetic activity of the Rubisco enzyme (McCarroll et al. 2003, Gagen et al. 2007, Porter et al. 2009). Therefore, temperature was expected to be the main factor affecting isotope values at the well-watered Hallormsstaður site, and this was confirmed by our analyses.

Studies of the climate sensitivity of tree-ring $\delta^{13}C$ and $\delta^{18}O$ of Sitka spruce are missing. Research on other coniferous trees have shown most frequently a positive correlation with annual or summer temperature, which is in agreement with our findings for Sitka spruce (Figure 4). Positive correlations of summer temperature with $\delta^{13}C$, $\delta^{18}O$ (or both) have been identified for: *Pinus sylvestris* in the French Alps (Gagen et al. 2004), Switzerland (Sauer et al. 2008) and Sweden (Esper et al. 2018); *Abies alba* and *Picea abies* in Switzerland and Germany (Sauer et al. 2008, Weigt et al. 2015); *Picea glauca* in North Canada (Porter et al. 2009); *Larix decidua* in the French and Swiss Alps (Daux et al. 2011, Esper et al. 2020); and *Pseudotsuga menziesii* in Germany (Weigt et al. 2015).

The most significant correlations between temperature and tree-ring parameters were relatively stable over time (Figure 4a). The decrease of the correlation observed between July-August temperature and TRWI at the end of the observation period may be related to the "divergence problem" (described in Brifa et al. 1998). A similar change of positive correlations with summer temperature for *Picea abies* in Norway has been found, when the positive effect of temperature lost its significance after 2000 (Čermák et al. 2019). Some possible explanations relate the divergence anomaly to a response to climate change. Changes in climatic parameters can be non-linear; different variables can have a different course of change. Tree-ring width might be controlled by variables other than average temperature, such as maximum and minimum temperatures (D'Arrigo et al. 2008).

Potential Sitka spruce for forestry in Iceland

Recent studies from Sweden and Iceland show that Sitka spruce grows much better (it has bigger volume production) than Norway spruce in Scandinavia (Tengberg 2005, Reynisson 2011). The high growth potential of Sitka spruce is also shown by individual-tree growth models based on data from permanent sample plots established by the Icelandic Forest Service between 1970 and 2020 (Heiðarsson et al. 2022). When considering its further use in plantings in Iceland, we must take into account some of its problematic properties. Sitka spruce can have a large capacity for spread, as found out Nygaard & Øyen (2017) for coastal Norway, and its stands provide poor habitats for native species of lichen, moss and vascular plants (Elmarsdottir et al. 2008, Bidne 2016). We can expect that some biotic risks will increase as the climate changes. Increasing winter temperatures can promote larger overwintering populations of insect pests – for example, green spruce aphid (*Elatobium abietinum*) – which is an important defoliating pest of Sitka spruce in Iceland, especially in the south and east coastal regions (Blöndal 1987, Day et al. 1998, Kuckuk et al. 2021). For the same reasons, an increase in the occurrence and voracity of some defoliators of other planted conifers can be expected as a result of the extension of the pest ranges towards the north, or the loss of regulatory factors limiting their outbreak areas (Netherer & Schopf 2010, Ammunét et al. 2012).

Our results confirmed a stable radial growth of Sitka spruce in Hallormsstaður, with an increase in the last ten years (Figure 3). As expected, its growth was mainly controlled by summer temperatures (Figure 4). Precipitation was characterised by high interannual variability, but due to its generally high level it did not have a significant effect on the growth of Sitka spruce (Figure 2. 5). Given the current climatic conditions, their expected trends in the future and the ecological amplitude of Sitka spruce, we can expect the species to continue its vital growth. It can also be assumed that low average temperatures in the summer months (especially in July), which increase the likelihood of a negative pointer year, will become less frequent due to advancing climate change. From this point of view, Sitka spruce still appears to be a suitable tree species for cultivation in Iceland. However, its growth potential and reactions to changing climate condition should be assessed again in a few decades, when more stands have reached the rotation age.

ACKNOWLEDGEMENT

The authors thank Inna Roshka and Josef Čáslavský for laboratory work on the determination of stable isotopes.

Disclosure statement: No potential conflict of interest was reported by the author(s).

Funding: The work was supported by the Establishing bilateral cooperation with Icelandic forest service (EHP-BF10-OVNKM-1-023-01-2018, EEA and NORWAY GRANTS 2014–2021).

REFERENCES

Ammunét T, Kaukoranta T, Saikkonen K, Repo T & Klemola T 2012. Invading and resident defoliators in a changing climate: cold tolerance and predictions concerning extreme winter cold as a range-limiting factor. *Ecological Entomology* 37(3), 212-220. https://doi.10.1111/j.1365-2311.2012.01358.x

Barbour MM & Farquhar GD 2004. Do pathways of water movement and leaf anatomical dimensions allow development of gradients in $H_2{}^{18}O$ between veins and the sites of evaporation within leaves? *Plant Cell & Environment* 27, 107-121. https://doi.10.1046/j.0016-8025.2003.01132.x

Barclay DJ, Wiles GC & Calkin PE 1999. A 1119-year tree-ring-width chronology from western Prince William Sound, southern Alaska. *The Holocene* 9(1), 79-84. https://doi.10.1191/095968399672825976

Bidne OGS 2016. Produksjon av sitkagran (*Picea sitchensis*) med omsyn til Naturmangfald-lova [Production of Sitka spruce (*Picea sitchensis*) with consideration of the Natural Diversity-Information Act. Bachelor thesis, Høgskolen i Hedmark] Retrieved from https://brage.inn.no/inn-xmlui/bitstream/handle/11250/2390987/Bidne.pdf?sequence=1 [In Norwegian].

Blöndal S 1987. Afforestation and reforestation in Iceland. *Arctic and Alpine Research* 19(4), 526-529.

Blöndal S & Gunnarsson SB 1999. Íslandsskógar. Hundrað ára saga. Reykjavík, Mál og mynd [Icelandic forests. A hundred years of history] Reykjavík, Matter and Image. [In Icelandic].

Brifa KR, Schweingruber FH, Jones PD, Osborn TJ, Shiyatov SG & Vaganov EA 1998. Reduced sensitivity of recent tree growth to temperature at high northern latitudes. *Nature*, 391, 678–682. https://doi.10.1038/35596

Cudlín P, Novotný R, Moravec I & Chmelíková E 2001. Retrospective evaluation of the response of montane forest ecosystems to multiple stress. *Ekológia* 20: 108–124.

Čermák P, Rybníček M, Žid T, Stefenrem A & Kolář T 2019. Site and age-dependent responses of *Picea abies* growth to climate variability. *European Journal of Forest Research* 138, 445–460. https://doi.10.1007/s10342-019-01182-6

D'Arrigo R, Wilson R, Liepert B & Cherubini P 2008. On the 'Divergence Problem' in Northern Forests: A review of the tree-ring evidence and possible causes. *Global and Planetary Change* 60(3–4), 289-305. https://doi.10.1016/j.gloplacha.2007.03.004

Daux V, Edouard JL, Masson-Delmotte V, Stievenard M, Hoffmann G, Pierre M, Mestre

O, Danis PA & Guibal F 2011. Can climate variations be inferred from tree-ring parameters and stable isotopes from *Larix decidua*? Juvenile effects, budmoth outbreaks, and divergence issue. *Earth and Planetary Science Letters* 309(3–4), 221-233. https://doi.10.1016/j.epsl.2011.07.003

Day KR, Halldórsson G, Harding S & Straw NA (eds.) 1998. The Green Spruce Aphid in Western Europe: Ecology, Status, Impacts and Prospects for Management. Forestry Commission Technical Paper 24. Retrieved from: https://cdn.forestresearch.gov.uk/1998/03/fctp024.pdf

Dombrosky J 2020. A ~1000-year 13C Suess correction model for the study of past ecosystems. *The Holocene* 30(3), 474-478. https://doi.10.1177/0959683619887416

Eggertsson O, Nygaard PH & Skovsgaard JP 2008. History of afforestation in the Nordic countries. Retrieved from https://www.researchgate.net/publication/237656493_History_of_afforestation_in_the_Nordic_countries

Elmarsdottir A, Fjellberg A, Halldorsson G, Ingimarsdottir M, Nielsen OK, Nygaard P, Oddsdottir ES & Sigurdsson BD 2008. Effects of afforestation on biodiversity. In: Halldorsson G, Oddsdottir ES & Sigurdsson BD (eds.) AFFORNORD. Effects of afforestation on ecosystems, landscape and rural development. TemaNord 562, Nordic Council of Ministers, Copenhagen, 37–47. Retrieved from: https://www.researchgate.net/publication/256648752_AFFORNORD_Effects_of_afforestation_on_ecosystems_landscape_and_rural_development/download [Accessed 16 January 2023]

Esper J, Holzkämpe S, Büntgen U,· Schöne B, Keppler F, Hartl C, Georges SS, Riechelmann DFC & Treydte K 2018. Site-specific climatic signals in stable isotope records from Swedish pine forests. *Trees* 32, 855-869. https://doi.10.1007/s00468-018-1678-z

Esper J, Riechelmann DFC & Holzkämper S 2020. Circumferential and Longitudinal $\delta^{13}C$ Variability in a *Larix decidua* Trunk from the Swiss Alps. *Forests* 11, 117. https://doi.10.3390/f11010117

Farquhar GD, Ehleringer R & Hubic KT 1989. Carbon isotope discrimination and photosynthesis. *Annual Review of Plant Physiology and Plant Molecular Biology* 40, 503-537.

Feliksik E & Wilczyński S 2008. Tree-ring chronology as a source of information on susceptibility of Sitka spruce to climatic conditions of Pomerania (northern Poland). *Geochronometria* 30, 79-82. https://doi.10.2478/v10003-008-0002-0

Feliksik E & Wilczyński S 2009. The Effect of Climate on Tree-Ring Chronologies of Native and Nonnative Tree Species Growing Under Homogenous Site Conditions. *Geochronometria* 33(1), 49-57. https://doi.10.2478/v10003-009-0006-4

Franklin JF & Dyrness CT 1973. Natural vegetation of Oregon and Washington. Gen. Tech. Rep. PNW-8. Portland, OR: U.S. Department of Agriculture, Forest Service, Pacific Northwest Forest and Range Experiment Station. 417 p. Retrieved from: https://www.fs.usda.gov/pnw/pubs/pnw_gtr008.pdf

Frigo D, Eggertsson O, Prendin AL, Dibona R, Unterholzner L & Carrer M 2023. Growth form and leaf habit drive contrasting effects of Arctic amplification in long-lived woody species. *Global Change Biology* 29, 5896-5907. Doi: 10.1111/gcb.16895

Gagen M, McCarroll D & Edouard JL 2004. Latewood width, maximum density, and stable carbon isotope ratios of pine as climate indicators in a dry subalpine environment, French Alps. *Arctic, Antarctic, and Alpine Research* 36, 166-171.

Gagen M, McCarroll D, Loader NJ, Robertson I, Jalkanen R & Anchukaitis KJ 2007. Exorcising the 'segment length curse': summer temperature reconstruction since ad 1640 using non-detrended stable carbon isotope ratios from pine trees in northern Finland. The *Holocene* 17, 435-446. https://doi.10.1177/0959683607077012

Government of Iceland 2020. Iceland's 2020 Climate Action Plan. Retrieved from: https://www.government.is/library/01-Ministries/Ministry-for-The-Environment/201004%20Umhverfisraduneytid%20Adgerdaaaetlun%20EN%20V2.pdf

Griffith RS 1992. *Picea sitchensis*. In: Fire Effects Information System, U.S. Department of Agriculture, Forest Service, Rocky Mountain Research Station, Fire Sciences Laboratory

(Producer). Retrieved from: https://www.fs.usda.gov/database/feis/plants/tree/picsit/all.html

Hannak N & Eggertsson O 2020. The long-term effects of climatic factors on radial growth of downy birch (*Betula pubescens*) and rowan (*Sorbus aucuparia*) in East Iceland. *Icelandic Agricultural Sciences* 33, 73-87. https://doi.10.16886/IAS.2020.07

Heiðarsson L, Pukkala T & Snorrason A 2022. Individual-tree growth models for Sitka spruce (*Picea sitchensis*) in Iceland. *Icelandic Agricultural Sciences* 35, 3-16. https://doi.10.16886/IAS.2022.01

Huang W, Fonti P, Larsen JB, Ræbild A, Callesen I, Pedersen NJ & Hansen JK 2017. Projecting tree-growth responses into future climate: A study case from a Danish-wide common garden. *Agricultural and Forest Meteorology* 247: 240-251. https://doi.10.1016/j.agrformet.2017.07.016

Kasesalu H, Läänelaid A, Roht U 2019. Sitka spruce in Estonia. Baltic Forestry 25(2): 296–302. Doi: 10.46490/vol25iss2pp296

Klinka K, Feller MC, Green RN, Meidinger DV, Pojar J & Worral J 1990. Ecological principles: applications. In: Lavender DP, Parish R, Johnson CM, Montgomery G, Vyse A, Winston D (eds.) Regenerating British Columbia's forests. Vancouver, BC: University of British Columbia Press: 55–72. Retrieved from: https://www.for.gov.bc.ca/hfd/pubs/docs/mr/mr063.pdf

Kuckuk J, van Manen S, Eggertsson O, Oddsdóttir ES & Esper J 2021. Defoliation and dieback of Sitka spruce in Reykjavík, Iceland. *Icelandic Agricultural Sciences* 34, 15-28. https://doi.10.16886/IAS.2021.02

Läänelaid A & Helama S 2019. Climatic Determinants of Introduced Sitka Spruce in Hiiumaa Island, Estonia. *Baltic Forestry* 25(1), 161-167. https://doi.10.46490/vol25iss1pp161

Levanič T & Eggertsson O. 2008. Climatic effects on birch (*Betula pubescens* Ehrh.) growth in Fnjoskadalur valley, northern Iceland. *Dendrochronologia* 25(3), 135-143. https://doi.10.1016/j.dendro.2006.12.001

McCarroll D, Jalkanen R, Hicks, S, Tuovinen M, Gagen M, Pawellek F, Eckstein D, Schmitt U, Autio J & Heikkinen O 2003. Multiproxy dendroclimatology: a pilot study in northern Finland. *The Holocene* 13, 829-838. https://doi.10.1191/0959683603hl668rp

Netherer S & Schopf A 2010. Potential effects of climate change on insect herbivores in European forests – General aspects and the pine processionary moth as specific example. *Forest Ecology and Management* 259(4), 831-838. https://doi.10.1016/j.foreco.2009.07.034

Nygaard PH & Øyen BH 2017. Spread of the introduced Sitka spruce (*Picea sitchensis*) in coastal Norway. *Forests* 8(24). https://doi.10.3390/f8010024

Ols C, Klesse S, Girardin MP, Evans MEK, DeRose RJ & Trouet V 2023. Detrending climate data prior to climate–growth analyses in dendroecology: A common best practice? *Dendrochronologia* 79, 126094. https://doi.10.1016/j.dendro.2023.126094

Opała-Owczarek M., Owczarek P, Phulara M, Bielec-Bąkowska Z & Wawrzyniak Z 2024. Dendrochronology and extreme climate signals recorded in seven Icelandic shrubs: A multi-species approach in the sub-Arctic. *Dendrochronologia*, 85, 126207. https://doi.10.1016/j.dendro.2024.126207

Palmer JG, Turney CSM, Fogwill C, Fenwick P, Thomas Z, Lipson M, Jones RT, Beaven B, Richardson SJ & Wilmshurst JM 2017. Growth response of an invasive alien species to climate variations on subantarctic Campbell Island. *New Zealand Journal of Ecology* 42(1). https://doi.10.20417/nzjecol.42.2

Pettitt AN 1979. A non-parametric approach to the change-point problem. *Applied Statist*ic 28, 126-135. https://doi.10.2307/2346729.

Piermattei A, Urbinati C, Tonelli E, Eggertsson O, Levanič T, Kaczka RJ, Andrew C, Schöne BR, Büntgen U 2017. Potential and limitation of combining terrestrial and marine growth records from Iceland. *Global and Planetary Change* 155, 213-224. https://doi.10.1016/j.gloplacha.2017.07.010

Porter TJ, Pisaric MFJ, Kokelj SV & Edwards TWD 2009. Climatic signals in $\delta^{13}C$ and $\delta^{18}O$ of tree-rings from white spruce in the Mackenzie Delta region, northern Canada. *Arctic, Antarctic,*

and Alpine Research 41(4), 497-505. https://doi.10.1657/1938-4246-41.4.497

Phulara M, Opała-Owczarek M & Owczarek P 2022. Climatic Signals on Growth Ring Variation in *Salix herbacea*: Comparing Two Contrasting Sites in Iceland. *Atmosphere* 13(5), 718. https://doi.10.3390/atmos13050718

Quinn GP & Keough MJ 2002. Experimental design and data analysis for biologists. Cambridge University Press, Cambridge, U.K. 537 p. https://doi.10.1017/cbo9780511806384

Reynisson V 2011. Comparison of yield of Norway spruce (*Picea abies*) and Sitka spruce (*Picea sitchensis*) in Skorradalur, West Iceland. Swedish University of Agricultural Sciences Master Thesis no. 168, Southern Swedish Forest Research Centre. 40 pp. Retrieved from: https://core.ac.uk/reader/11987680

Römer P, Reinig F, Konter O, Friedrich R, Urban O, Čáslavský J, Pernicová N, Trnka M, Büntgen U & Esper J 2023. Multi-proxy crossdating extends the longest high-elevation tree-ring chronology from the Mediterranean. *Dendrochronologia* 79: 126085. https://doi.10.1016/j.dendro.2023.126085

Saurer M, Cherubini P, Reynolds-Henne CE, Treydte KS, Anderson WT & Siegwolf RTW 2008. An investigation of the common signal in tree ring stable isotope chronologies at temperate sites. *Journal of Geophysical Research* 113, G04035. https://doi.10.1029/2008JG000689

Sigurdsson BD & Snorrason A 2000. Carbon sequestration by afforestation and revegetation as means of limiting net-CO_2 emission in Iceland. *Biotechnology, Agronomy, Society and Environment* 4(4), 303-307.

Snorrason A, Kjartansson BÞ, Gunnarsson E & Eysteinsson T 2005. Global Forest Resources Assessment Update 2005. Iceland. Country Report. FAO. 50 pp.

Snorrason A, Sigurdsson BD, Guðbergsson G, Svavarsdóttir K & Jónsson ÞH 2002. Carbon sequestration in forest plantations in Iceland. *Icelandic Agricultural Sciences* 15, 81-93. Retrieved from. https://citeseerx.ist.psu.edu/document?repid=rep1&type=pdf&doi=c8742462eff387a0d1ed664de3e1b56794515c6a

Tengberg F 2005. En Jämförelse av sitkagranens (*Picea sitchensis*) och den vanliga granens (*P. abies*) production. . [A comparison of sitka spruce (*Picea sitchensis*) and common spruce (*P. abies*) production] Institutionen för sydsvensk skogsvetenskap Alnarp, Sveriges Lantbruksuniversitet, examensarbete nr 62. Retrieved from: https://stud.epsilon.slu.se/11638/1/tengberg_f_171002.pdf [In Swedish]

Urban O, Ač A, Kolář T, Rybníček M, Pernicová N, Koňasová E, Trnka M & Büntgen U 2021. The dendroclimatic value of oak stable isotopes. *Dendrochronologia* 65, 125804. https://doi.10.1016/j.dendro.2020.125804

Vihermaa LE 2010. Influence of site factors and climate on timber properties of Sitka spruce (*Picea sitchensis* (Bong.) Carr.). PhD thesis. Retrieved from: http://theses.gla.ac.uk/2271/

Weigt RB, Bräunlich S, Zimmermann L, Saurer M, Grams TEE, Dietrich HP, Siegwolf RTF & Nikolova PS 2015. Comparison of $\delta^{18}O$ and $\delta^{13}C$ values between tree-ring whole wood and cellulose in five species growing under two different site conditions. *Rapid Communication Mass Spectrometry* 29, 2233-2244. https://doi.10.1002/rcm.7388

Wiles GC, D'Arrigo RD & Jacoby GC 1998. Gulf of Alaska atmosphere-ocean variability over recent centuries inferred from coastal tree-ring records. *Climatic Change* 38: 289-306. https://doi.10.1023/A:1005396027562w

Received: 14.2.2024
Accepted 11.6.2024

www.ias.is
https://doi.org/10.16886/IAS.2024.03 ICEL. AGRIC. SCI. 37 (2024), 25-37

Models for simulating the temporal development of black cottonwood (*Populus balsamifera* L. ssp. *trichocarpa* (Torr. & Gray ex Hook.) Brayshaw) plantations in Iceland

Lárus Heiðarsson[1], Timo Pukkala[2] and Arnór Snorrason[1]

[1]Land and Forest Iceland, Mógilsá, IS-116 Reykjavík, Iceland
(larus.heidarsson@landogskogur.is , arnor.snorrason@landogskogur.is)
[2] University of Eastern Finland, P.O.Box 111, 80101 Joensuu, Finland (timo.pukkala@uef.fi)

ABSTRACT

Black cottonwood (*Populus balsamifera ssp. trichocarpa)* was initially introduced to Iceland in 1944 from the Kenai Peninsula in Alaska and has been widely planted in shelterbelts and afforestation projects since the 1980s. There is currently much interest in increasing the planting of black cottonwood, especially in carbon sequestration projects, because of its rapid growth at an early age. Growth models simulate the growth of a forest over time and are important tools for forest managers, researchers, and policymakers. This study presents, for the first time, site index, individual-tree diameter increment and tree height models for even-aged black cottonwood stands in Iceland. The data were collected from Icelandic national forest inventory (NFI) plots and from three plots from a network of permanent sample plots (PSP). The NFI data were collected during 2005–2022, and the PSP data were collected between 2009 and 2022. The model of McDill and Amateis was selected for predicting site index and dominant height development, and the model of Schumacher was selected for predicting tree height. For diameter increment modelling, an optimization-based modelling approach was found to be more suitable than non-linear regression analysis. The models developed in this study can be used in forestry practice and in optimization studies for thinned black cottonwood stands. The models produced simulation results that corresponded to measured stand development.

Keywords: Growth model, individual-tree model, optimization-based modelling, plantation forestry

YFIRLIT

Jöfnur sem lýsa vexti alaskaaspar (Populus balsamifera L. ssp. trichocarpa) *á íslandi.*

Alaskaösp var fyrst flutt til landsins frá Kenai í Alaska árið 1944 og hefur verið mikið notuð í skjólbelta- og skógrækt frá 1980. Í dag er mikill áhugi á aukinni notkun á alaskaösp, sérstaklega í kolefnisverkefnum vegna hraðs vaxtar snemma á æviskeiðinu. Vaxtarjöfnur spá fyrir um framtíðarvöxt skóga og eru mikilvæg verkfæri fyrir skógarstjórnendur, vísindamenn og stefnumótendur fyrir ákvarðanartöku, meðal annars í loftslagsmálum. Í þessari rannsókn eru birtar í fyrsta sinn jöfnur sem lýsa gróskustigi, þvermálsvexti og hæðarvexti trjáa fyrir jafnaldra alaskaasparskóga á Íslandi. Gögnin sem notuð voru í rannsókninni eru trjámælingar, aðalega frá Íslenskri skógarúttekt (ÍSÚ) en þrír af mæliflötunum eru fastir mælifletir (FMF). Gögnunum úr ÍSÚ var safnað á árabilinu 2005–2022 og gögnunum frá FMF var safnað á árabilinu 2009–2022. Til að spá fyrir um gróskustig og yfirhæðarvöxt skóga var valin aðlöguð jafna sem gerð var af McDill og Amateis og til að spá fyrir um hæðarvöxt stakra trjáa var valin aðlöguð jafna gerð af Schumacher. Til að spá fyrir um þvermálsvöxt trjáa var notuð bestunarnálgun (optimization approach) en hún gaf nákvæmari niðurstöðu en blönduð aðhvarfsgreining

(mixed-effect modelling). Jöfnurnar sem aðlagaðar voru að íslenskum aðstæðum í þessari rannsókn má nota til áætlanagerðar og arðsemisútreikninga í grisjuðum alaskaasparskógum. Áætlaður vöxtur með jöfnunum er samsvarandi vexti viðkomandi skóga.

INTRODUCTION

Today, black cottonwood (*Populus balsamifera* L. ssp. *trichocarpa* (Torr. & Gray ex Hook.) Brayshaw) is an important tree species in Icelandic forestry, covering an area of 3900 ha, or 7% of the cultivated forest in Iceland (data from the Icelandic National Forest Inventory, NFI). The species was initially introduced to Iceland in 1944 from the Kenai Peninsula, Alaska (Bragason 1995). Black cottonwood has become an important urban tree in Iceland and has been widely planted in shelterbelts and afforestation projects since the 1980s (Óskarsson et al. 1990, Sigurdsson 2001a). In Iceland, there is currently much interest in increasing the planting of black cottonwood, especially in carbon sequestration projects, because of its rapid growth at an early age.

No growth models exist for black cottonwood in Iceland today, and scientific knowledge regarding its growth, yield and management is scant. The main reason for the lack of models is the young age of Icelandic black cottonwood plantations. A few recently published growth studies on black cottonwood focused on diameter growth, biomass and density (Eggertsson 2019, Mikaelsson 2011, Jóhannsdóttir 2012), or on fertilising and economic profit of short rotation forestry (Bogason et al. 2018).

In the last decade, the development of tree growth models has been ongoing in Iceland (Heiðarsson & Pukkala 2012, Heiðarsson et al. 2022, Heiðarsson et al. 2023). Growth models simulate the growth of a forest over time and are important tools for forest managers, researchers, and policymakers. They help to optimize forest management, such as thinning and harvesting, to maximize timber production or economic return while minimizing environmental impacts (Weiskittel 2014). Advanced models can be used to predict the effects of climate change on forest growth. Model integration makes it possible to develop forest management strategies that mitigate the harmful effects of climate change, while providing timber for forest industries and income for forest landowners (Heinonen et al. 2018, Trouillier et al. 2020).

Generally, a growth model refers to a system of equations that predict the growth and yield of a forest stand under a wide variety of conditions (Vanclay 1994). Growth models can be divided into three broad categories: stand-level models, individual-tree models, and diameter distribution models (Munro 1974). Stand-level models are developed using stand-level information (Curtis et al. 1981, Vanclay 1994), whereas individual-tree models predict individual tree growth or mortality (Clutter et al. 1983, Palahí & Pukkala, 2003). Diameter distribution models use statistical probability density functions to characterize the stand structure (Bailey & Dell 1973, Newton et al. 2005). Tree-level models are further classified as distance-dependent (spatial) or distance-independent (non-spatial) models.

The recent trend in Iceland has been to develop distance-independent individual tree models (Heiðarsson & Pukkala 2012, Heiðarsson et al. 2022, Heiðarsson et al. 2023). This type of model was targeted also in the current study because the available data contained no spatial information. The model set we developed for black cottonwood consists of a site index (SI) model (top height growth model), a tree height model, and an individual tree model for diameter increment. We provide below the rationale for the development of these three models.

For even-aged monocultures, SI models are the most common tools for estimating site productivity. SI is defined as the dominant height, i.e. the average height of the 100 largest trees per hectare, at a chosen reference age (Monserud 1984, Skovsgaard & Vancley 2008, Burkhart & Tomé 2012). For most tree species, the height growth of dominant and co-

dominant trees in a stand is a stable predictor of site quality, because it is not much affected by stand density or thinning operations, assuming thinning from below (Cieszewski & Bella 1989, Skovsgaard & Vancley 2008, Weiskittel et al. 2009, Burkhart & Tomé 2012). SI models are widely used in forestry practice and research, due to the strong correlation between stand height and volume production (Vancley 1994, Skovsgaard & Vancley 2008).

Information on tree heights is essential in forest inventories for computing tree volumes. Tree height information is also needed in growth and yield simulators (Mehtätalo et al. 2015). Because field measurements of tree height are rather time-consuming and therefore expensive, many forest inventories use predictive models to get height estimates for the trees based on their diameter.

Tree diameter increment is an important metric for estimating wood production and can be easily measured in inventories. Stand management decisions, such as when and how much to thin a stand, rely heavily on variables derived from tree diameters. The development of models for diameter increment usually employs data from permanent plots, in which all trees have been remeasured at regular intervals (Juma et al. 2014).

To achieve the above, there is a reasonable number of repeated measurements available on black cottonwood plots for various regions of Iceland. The datasets currently available include mainly younger stands between 10 and 30 years in age. In these datasets, there is only one unthinned control plot and a few plots in which the planting density deviates from normal densities.

This study aimed to develop a set of models for site index, tree height and diameter increment to predict the yield of black cottonwood plantations in Iceland. Because of the young age of the measured stands, these models should be looked at as preliminary, their main purpose being growth estimation in young stands over a short period of time.

MATERIAL AND METHODS

Sample plot data

The data used for black cottonwood (*Populus balsamifera* L. ssp. *trichocarpa* (Torr. & Gray ex Hook.) Brayshaw) stands in this study were mainly collected from Icelandic national forest inventory plots (NFI). The NFI data are a statistical sample of all forested land areas in Iceland. Three plots of the dataset are permanent sample plots (PSP) established by Land and Forest Iceland for growth measurements. The NFI data were collected during 2005–2022 and the PSP data were collected between 2009 and 2022. The NFI data were collected from 14 permanent plots in 14 locations. The PSPs were measured in two locations (Figure 1). All plots are in planted, even-aged black cottonwood stands, established by Land and Forest Iceland. The NFI plots were remeasured with 5-year intervals and included 42 growth periods (Table 1). Two of the PSP plots were measured annually, and one had a 9-year interval between measurements.

The dataset covered different site types and growth conditions, mainly from young stands. All the locations have an oceanic climate with an annual precipitation (1964–1990) of 700–1200 mm and a mean annual temperature of 3.2–4.5°C (Vedurstofa Islands 2017). For the same period, the mean maximum daytime temperature during June–August was 12.9–13.6 °C (Vedurstofa Islands 2017). The range in plot elevation was between 10 and 140 m a.s.l.

The sample plots were circular, and the size of the plots varied between 0.01 and 0.02 ha. On every measurement occasion, the diameter at breast height (DBH, at 1.3 m) was measured on all trees that had reached that height. On some of the NFI plots, the total tree height was measured only on sample trees. The tree selection for height measurements was based on DBH, and the aim was to get heights from different DBH classes. Height was measured with a measuring pole for trees shorter than 4 m and with Vertex Laser VL5 and Laser Tech distance and height measurement instruments for taller trees. Because of the young age of the sampled forests, there was no mortality in the

Table 1. Mean, standard deviation (SD) and range of the main characteristics of the study material on black cottonwood in Iceland. N: number of observations; DBH: diameter at breast height; Growth: 5-year DBH growth; G: stand basal area; Age: stand age; Hdom: dominant height.

Variable	N	Mean	SD	Maximum	Minimum
DBH (cm)	813	6.15	4.86	39.0	0.0
Height (m)	737	4.74	2.88	23.4	0.31
Growth (cm)	813	2.81	1.73	10.4	0.1
G (m^2ha^{-1})	42	7.58	11.09	45.6	0.01
Age (years)	42	21.9	6.59	48.0	12.0
Hdom (m)	42	6.26	3.88	23.2	2.07
Growth periods	42	5.0	0	9.0	1.0
Stems per hectare	42	1524	928	4400	400

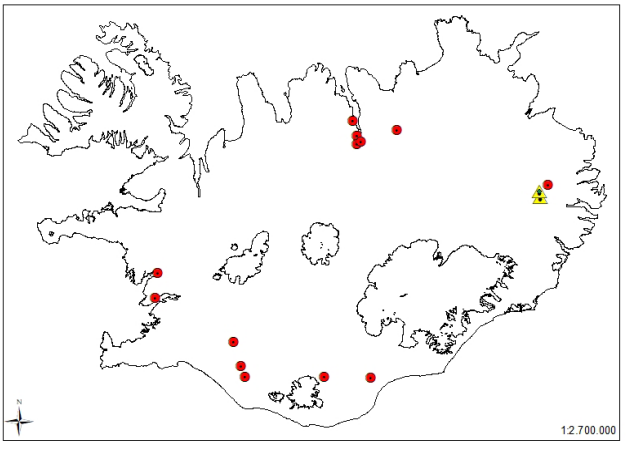

Figure 1. Geographical locations of the study sites in Iceland. The red dots present the NFI plots, and the yellow triangles are PSP plots.

dataset, and no attempt was made to model tree survival. All regression models were fitted with the R software, version 4.3.1 (Posit team 2023).

Site index modelling

Two datasets were tested in the site index modelling: one with only first and last height measurements and one with all height measurements. Several functions commonly used in the algebraic difference approach (ADA) were tested (Palahí et al. 2004). The tested functions were: Korf and Lundmark (Korf 1939), Schumacher (1939), Chapman-Richards (Richards 1959) and the model of McDill and Amateis (1992). All models predict the dominant height H_2, at a certain time point T_2, using current dominant height H_1 and current age T_1 as predictors:

$$H_2 = f(T_1, H_1, T_2) + \varepsilon \qquad (1)$$

When T_1 is replaced by index age and H_1 is replaced by site index (dominant height at index age), the model gives the dominant height at age T_2 for site index H_1. If H_1 is the measured dominant height at age T_1 and T_2 is the index age, the model gives the site index. The index age was taken as 50 years, which has been previously used for black cottonwood in Alaska (Shaw & Packee 1998). Therefore, the site index is defined to be the dominant height of the stand at the age of 50 years.

Of the tested models, McDill and Amateis (1992) was selected for predicting site index and dominant height development.

$$H_2 = \frac{a_0}{1-\left(1-\frac{a_0}{H_1}\right)\times\left(\frac{T_1}{T_2}\right)^{a_1}} + \varepsilon \qquad (2)$$

where H_1 and T_1 are, respectively, dominant height and stand age at the first measurement, H_2 and T_2 are the same variables at the second measurement, a_0 and a_1 are parameters to be estimated and ε is the random error term of the equation.

Tree height modelling

The number of height observations available for individual tree height modelling was 737. Based on the study of Mehtätalo et al. (2015), the following models were tested: Näslund (1937), Schumacher (1939) and Curtis (1967). These

models were the best among the 28 datasets tested in that study. As the first step, fixed-effect models were fitted. Then the models were further developed by adding random plot factors to the fixed parameters and the models. The best combination of random plot factors was obtained by testing all possible combinations. Finally, the model of Schumacher (1939) was selected for predicting tree height.

$$h = 1.3 + (a_0 + a_1 H_{dom}) \times \exp\left[\frac{-\{b_0 + b_1 H_{dom}\}}{d}\right] + \varepsilon \quad (3)$$

where h is the tree height, H_{dom} is the dominant height, d is DBH, a_0, a_1, b_0, b_1 are fixed parameters to be estimated. The estimated parameters of the height model were modelled as a function of dominant height, which allowed the height curve to change along stand development.

Diameter increment modelling

Two different methods were tested to fit the models for diameter increment: non-linear regression analysis and the optimization-based approach suggested by Pukkala et al. (2011) and used earlier in Iceland by Heiðarsson et al. (2022) for Sitka spruce and Heiðarsson et al. (2023) for lodgepole pine. The model had to include at least one predictor for each of the following three influences: tree size, competition, and site productivity. Tree size was described by DBH and its transformations, and the site index was used to describe the effect of site productivity. To describe competition, stand basal area and basal area in trees larger than the subject tree were tested.

As the first step, regression analysis and mixed-effect modelling were used to search for the best transformations and combinations of predictors for the model. The following model turned out to be the most satisfactory:

$$i_{\mathrm{DBH}} = \exp\left(a_0 + a_1 lnd + a_2\left(\frac{d}{10}\right)^2 + a_3 G + a_4 lnSI + a_5\left(\frac{BAL}{\sqrt{d+1}}\right)\right) + \varepsilon \quad (4)$$

where i_{DBH} is the diameter increment (cm), d is DBH (cm), G is the stand basal area (m^2ha^{-1}), SI is the site index (m), and BAL is the basal area in larger trees than the subject tree (m^2ha^{-1}).

The predicted variable in regression analysis was a five-year diameter increment. Tests with the regression model suggested that the model may overestimate diameter increment in long-term simulations if the stand is not thinned. The probable reason for this outcome was that the modelled effect of increasing basal area on diameter increment was not strong enough, i.e. regression analysis resulted in a too flat relationship.

In two sample plots, tree diameters were measured annually over six years. These plots allowed us to see that the annual diameter increment may decrease substantially during a five-year measurement interval, most probably because of increased competition (Figure 2).

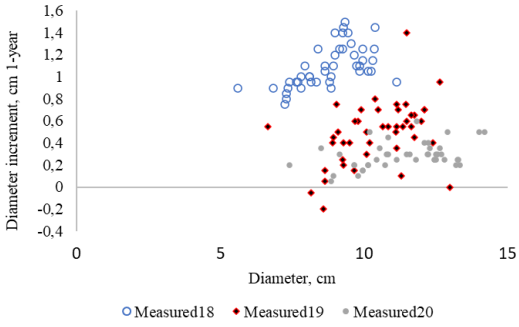

Figure 2. Relationship between diameter increment and tree diameter in the first, third, and fifth year of a five- year period in a plot where tree diameters were measured annually (at age 18, 19 and 20 years) for black cottonwood in Iceland.

To fully utilize the annually measured data from the two plots and to improve the modelled relationship between competition and diameter increment, the model was refitted using the optimization-based approach of Pukkala et al. (2011). In this model, the predicted variable of the model was annual diameter increment.

In the optimization-based approach, the tree diameters of the first measurement are used to start a simulation where tree growth is simulated

from the first measurement to the second, using a one-year time step. The parameters of the diameter increment model are gradually adjusted, by using an optimization algorithm, so that the simulated diameter distribution at the end of the measurement interval corresponds to the measured diameter distribution of the trees.

The method minimizes a loss function, which describes the difference between the simulated and measured diameter distribution. The loss function used both the distribution of basal area and the distribution of the number of trees into different diameter classes. The minimized loss function was as follows:

$$\min z(\theta) = \sum_{k=1}^{K}\left[\sum_{j=1}^{J_k} w_{jk} \sum_{i=1}^{I_j} \left|g_{ijk}^{m} - g_{ijk}^{s}(\theta)\right| + 0.001\left|n_{ijk}^{m} - n_{ijk}^{s}(\theta)\right|\right] \quad (5)$$

where Θ is the set of coefficients (a_0,… a_5 of Equation 4) estimated as arg min z(Θ), K is the number of plots, J_k is the number of measurement intervals of plot k, I_j is the number of 3-cm diameter classes in measurement interval j of plot k, g_{ijk}^{m} and $g_{ijk}^{s}(\Theta)$ are, respectively, measured and simulated cumulative basal area (m^2ha^{-1}) of diameter class i at the end of measurement interval j of plot k, and n_{ijk}^{m} and $n_{ijk}^{s}(\Theta)$ are, respectively, the measured and simulated cumulative number of trees per hectare in diameter class i at the end of measurement interval j of plot k (see, e.g., de-Miguel et al. 2014 for details). Symbol w_{jk} is a weight. The number of trees in plot k at the beginning of period j was used as the weight.

The optimization-based modelling does not produce direct information on the reliability of the coefficients. Therefore, bootstrapping (Varian 2005, Jin et al. 2019) was employed to find out how much the coefficients vary in repeated model fittings which are based on different samples. The model was fitted 30 times, using random sampling with replacement. The sample size was the same as the true number of measurement intervals, but the same measurement interval could be selected more than once, and some measurement intervals may not be selected for the sample.

RESULTS

Site index model

Of the tested site index models, the model of McDill and Amateis minimized the RMSE and the Akaike Information Criterion. Most of the models tested predicted the dominant height development similarly, but the behaviour of the selected model outside the age and dominant height range of modelling data was evaluated to be the most logical for the model of McDill and Amateis. Model versions based on all observations vs. the first and the last observation of each plot were almost identical (Figure 3). The model based on the first and last top height measurement is as follows:

$$\widehat{SI} = \frac{40.0182}{1-(1-40.0182/H_{\mathrm{dom}})} \times \left(\frac{T}{50}\right)^{1.4276} \quad (6)$$

Both parameters were significant at the 0.01 level. The coefficient of determination was 0.84 and the RMSE was 1.04 m.

When site index and stand age are known, the model can be used to calculate the dominant height for certain site index: H_{dom} is replaced by SI, stand age T is replaced by 50 (index age), and 50 is replaced by stand age:

$$\widehat{H_{\mathrm{dom}}} = \frac{40.0182}{1-(1-40.0182/SI)} \times \left(\frac{50}{T}\right)^{1.4276} \quad (7)$$

Figure 3 shows that the model followed the patterns of the measured dominant heights of the sample plots used in this study.

According to the model, the dominant height growth reached the maximum at different ages, depending on site productivity (Figure 4). For site index SI 25 and SI 20, the maximum was reached between 10 and 15 years, for site index SI 15 between 20 and 25 years and site index SI 10 between 30 to 35 years. At the age of 50 years, the annual dominant height growth was 0.3 meters or less in all site indices.

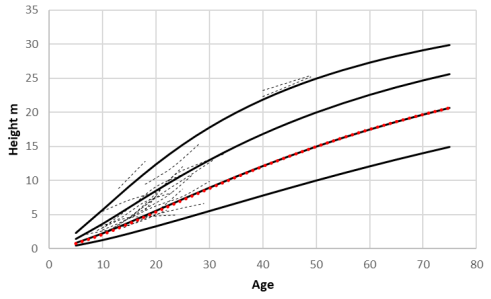

Figure 3. Dominant height curves for black cottonwood in Iceland (thick black lines) for site indices 10, 15, 20 and 25 m (site index = dominant height at 50 years) and the measured age and dominant height sequences of the study plots (thin dashed lines). The red dotted curve is the prediction for site index 15 based on the fixed part of a mixed-effects model that was fitted using all dominant height measurements of the dataset.

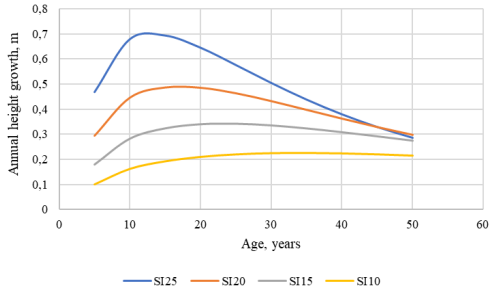

Figure 4. Annual height growth for different site indices (SI) for black cottonwood in Iceland. From above SI25, SI20, SI15 and at the bottom SI10 (site index = dominant height at 50 years).

Tree height model

The Schumacher model for tree height was as follows:

$$\hat{h} = 1.3 + (0.0543 + u_{0k}) + (1.1594 + u_{1k})H_{\text{dom}}) \times \exp\left[-\frac{(0.9747+0.4058H_{\text{dom}})}{d}\right] \quad (8)$$

where is the tree height, H_{dom} is the dominant height, d is DBH, and u_{0k}, and u_{1k} are random factors for plot k (Table 2).

The standard deviation of the residuals (RMSE) for the mixed-effect model (when the random effects are used in prediction) was 0.46 m (Table 2). When the tree height predictions were calculated with the fixed part of the mixed-effect model (assuming that the random effects are zero), the RMSE was 0.62 m. The bias of the fixed part of the mixed-effect model was –0.048 m, i.e. the model underestimated tree height on average by 4.8 cm, which is not substantial. All parameters except a_0 were significant at the 0.001 level, and the residuals were normally distributed with a constant variance at different diameters (Figure 5). Figure 6 shows that the tree diameter-height curve rose when the stand developed.

Table 2. Standard deviations and correlations of the random plot effects of the height model for black cottonwood in Iceland (Equation 8).

Standard deviations		Correlations	
u_{0k}	1.040	u_{0k}	u_{0k}
u_{1k}	0.103	u_{1k}	-0.579
Residual	0.455		

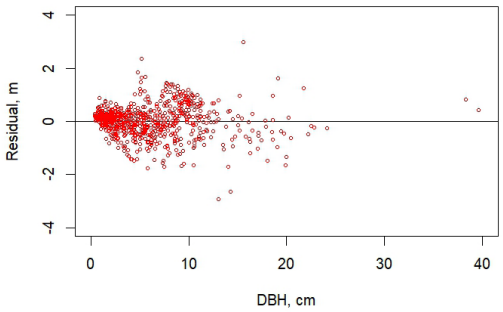

Figure 5. Residuals (observed-predicted) in predicting tree height with the fixed part of the mixed model for black cottonwood in Iceland.

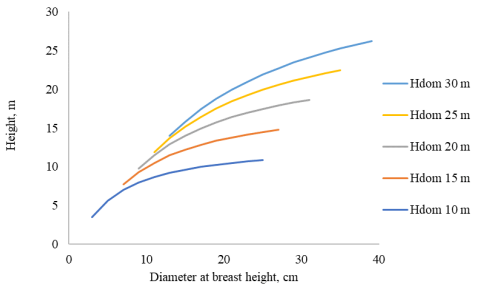

Figure 6. Relationship between diameter at breast height and tree height at different dominant heights (Hdom) for black cottonwood in Iceland.

Diameter increment model

The diameter increment model, fitted with the optimization-based approach, was as follows:

$$\widehat{\iota_{\mathrm{DBH}}} = \exp\left(-6.5902 + 0.5963\ln d - 0.1213\left(\frac{d}{10}\right)^2 - 0.0213G + 1.8793\ln SI - 0.1359\left(\frac{BAL}{\sqrt{d+1}}\right)\right) \quad (9)$$

where $\widehat{\iota_{\mathrm{DBH}}}$ is the future 1-year diameter increment (cm), d is the DBH (cm), G is the stand basal area (m^2ha^{-1}), SI is the site index (m) and BAL is the basal area in trees larger than the subject tree (m^2ha^{-1}). The bootstrap analysis suggested that all parameters of the model were significant (Table 3). The bias of the periodical basal area increment of the plot was 0.21 m^2ha^{-1}, which is 4.3% of the measured basal area increment. This means that the model slightly underestimated growth. The relative RMSE of the periodical plot-level basal area increment was 39%.

Figure 7 (top) shows the predicted diameter increment for different diameters and site indices when the stand basal area is constant and BAL decreases with increasing DBH. Figure 7 (top) indicates how trees of different DBHs would grow in an even-aged stand. The model predicted that the largest trees of the stand grow best, implying that the DBH differences between the smallest and the largest trees would increase with time.

Figure 7 (bottom) shows the effect of competition on diameter increment, with DBH set at 15 cm and BAL at 50% of the stand basal area. The diagram shows the strong negative effect of increasing stand density on DBH increment.

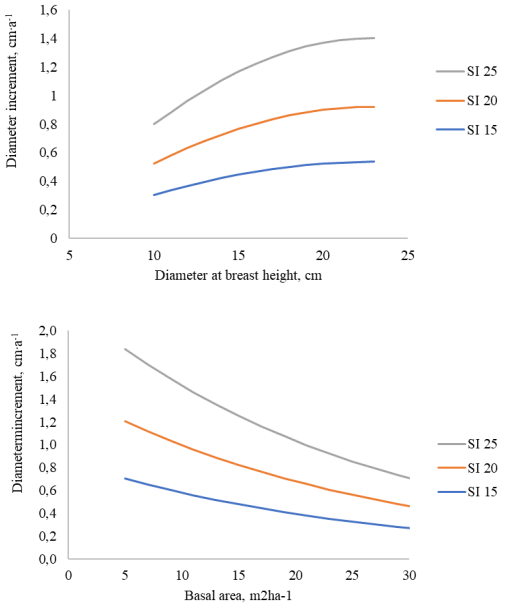

Figure 7. Top: Predicted diameter increment in an even-aged stand of black cottonwood in Iceland where DBH ranges from 10 to 23 cm, basal area is constant (15 m^2ha^{-1}) and BAL decreases from 15 to 0 m^2ha^{-1} when DBH increases from 10 to 23 cm. Bottom: Diameter increment with different stand basal areas when DBH is 15 cm and BAL is 50% of the stand basal area.

Simulation examples

The diameter increment model was used to simulate the development of four plots of the dataset in Icelandic black cottonwood plantations with different site indices and stand basal areas (Figure 8). In general, the models predicted basal area increments that were close to the measured basal areas (basal areas calculated from DBH measurements). However,

Table 3. Bootstrapping results for the significance of the coefficients of the optimization-based diameter increment model for black cottonwood in Iceland. The bootstrapping results are based on 30 model fittings using random sampling with replacement. Sdev is the standard deviation.

Parameter	a_0	a_1	a_2	a_3	a_4	a_5
Mean	-6.6767	0.5329	-0.10069	-0.02169	1.9454	-0.1330
Standard deviation	0.0993	0.0331	0.0110	0.0010	0.0374	0.0052
"t" Mean/Sdev	-67.23	16.10	-9.16	-22.49	52.08	-25.55

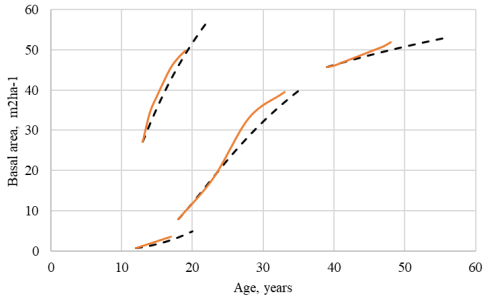

Figure 8. Examples of observed (continuous lines) and simulated (dashed lines) basal area development in four plots of the modelling dataset for black cottonwood in Iceland.

in one plot the model predicted slower growth rates than was measured. Also in this plot, the growth was predicted well for the first five years, from age 18 to age 23 years, but thereafter the measured growth was faster than the model prediction.

Residuals of observed vs. predicted values of DBH and BAL development from the two plots that were measured annually over six years are shown in Figure 9. The residuals of the model show that predictions for these two plots were unbiased, and there were no linear trends between the residuals and DBH or BAL. However, the scatter plots for DBH show a decreasing–increasing pattern, which may be explained, for example, by climate-induced annual variation in diameter increment. Figure 9 shows the residuals only for two out of 14 plots. When alternative models were tested with the full dataset, no transformations of DBH were found that resulted in better models than the one shown in Equation 9.

DISCUSSION

This study presents, for the first time, site index, individual tree diameter increment and tree height models for even-aged black cottonwood stands in Iceland. The available data for the growth modelling were mainly from NFI plots, which were not established for modelling purposes. As can be seen in Table 1 and Figure 3, the dataset is mainly from young stands between 10 and 30 years of age. The oldest stand was only 48 years old at the end of the measurement period. There was no mortality in the dataset, and data from very dense stands were lacking. The lack of mortality modelling limits simulations for stands older than 30 years and stands with high basal area (over 45 m^2ha^{-1}). Mikaelsson (2011) showed that survival rate is affected by high basal area.

The selection of the site index model was based on biological consistency, such as the value of the asymptote, on biological realism of the site index curves when compared with the modelling data, and on the behaviour of the model outside the age and dominant height range of modelling data (Figure 3). Figure 3 shows that the developed dominant height model resembles well the trends in the modelling data. The asymptote parameter of the dominant height model was 40 m, implying that the dominant height continues to grow at a rather

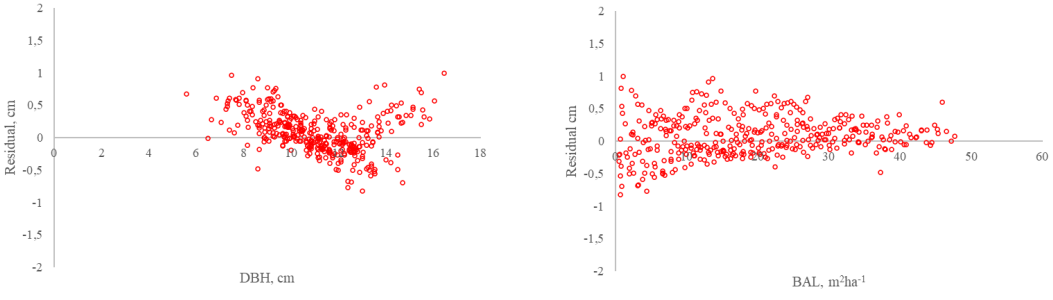

Figure 9. Residuals of the diameter increment model plotted against DBH and BAL in two plots where diameter increments were measured annually over six years.

old age. Forty meters is a realistic asymptote since black cottonwood trees can reach that height in favourable environments (Shaw & Packee 1998). In Iceland, the species is already approaching 30 m height at the oldest sites that were planted in the most favourable conditions (B.D. Sigurdsson, personal information). For stands younger than 10–20 years the site index curves should also be used with caution, because the height growth in younger stands is also affected by factors other than site index (Borders et al. 1984, Barrio Anta & Dieguez-Aranda 2005).

For site index SI 25 and SI 20, the maximum dominant height growth for black cottonwood occurs between 10 and 15 years (Figure 4). For site index SI 15, the maximum growth rate is reached between 20 and 25 years, and for site index SI 10 between 30 to 35 years. This is later than in Siberian larch (*Larix sibirica*), which is another pioneer species used in afforestation in Iceland (Heiðarsson & Pukkala 2012). At the age of 50 years, the annual dominant height growth rate of black cottonwood is 0.3 meters or less in all site indices, which is a realistic finding.

The tree height model is useful not only in yield simulators but also in predicting individual tree heights in field inventories when heights are not measured for all trees. As can be seen in Figure 5, the fit of the model is good, with no obvious trends or biases in the residuals. The selected tree height model guarantees that the simulated height development of individual trees is logically related to the dominant height development of the stand.

The height model was fitted as a mixed-effects model, which makes it possible to calibrate the model for a particular stand or plot. Simulations for volume development (not shown) suggested that, in most plots, the calibration had only a negligible effect on the simulation results, as compared to simulations where the random parameters were assumed to be zero. However, there were a few plots in which the full model provided better simulation results than the fixed part of the mixed-effect model. Therefore, model calibration is recommended whenever height measurements are available from the stand (Temesgen et al. 2008, de-Miguel et al. 2013).

The first step in diameter increment modelling was to search for the best transformation and combinations of predictors. Because the dataset has a hierarchical structure (correlations among observations), mixed-effect modelling was used for parameter estimation. When testing the mixed-effects model in longer-term simulations beyond the range of the data, the model seemed to result in overestimated basal area growth in dense unthinned stands. One reason for this outcome could be that the modelled effect of increasing basal area on diameter increment was not strong enough. Another reason was the lack of a mortality model. The problem of overestimated growth of unthinned stands was mitigated by using an optimization-based modelling approach (Pukkala et al. 2011). This approach was able to fully utilize the annual diameter measurements of some plots, which revealed the decreasing diameter increment with increasing stand basal area. Still, the models should be used with caution in denser stands. The optimization-based modelling approach can estimate also plot-specific coefficients to account for correlated observations (Juma et al. 2014), but they were considered unnecessary due to the preliminary nature of the models of this study.

Simulated basal area increments were compared to measured diameter increments in a few plots (Figure 8). The simulated increments were very close to the measured ones, with a small tendency of underestimation. One reason for the deviations seen in Figure 8 could be true changes in site index, which may be related, for example, to improved soil properties because of planted trees or to sheltering effects of a denser stand as it fills up the growing space. In the plot where the model started to underestimate growth after 10 years, the site index was 16.5 meters at the first measurement occasion, but 5 years later it was already 20.7. However, in simulations, the site index was kept constant. In Iceland, trees are planted in treeless lands, which are often used as pastures. Planted trees may have a favourable

effect on the site productivity. For example, trees produce litter, which may improve the soil due to the increased content of organic matter. It is also possible that tree roots gradually reach nutrient-rich or moister soil layers. Such an effect on height growth has been shown to occur in initial spacing experiments in Iceland planted in treeless landscapes (Jóhannsdóttir 2012). Because of these unique conditions of the Icelandic tree plantations, the site index estimates should not be regarded as permanent descriptions of site productivity. They should be updated every few years.

Tree growth depends on environmental variables like climate and soil. Therefore, annual variation in environmental variables, such as temperature and precipitation, can alter annual growth rates, which is e.g. utilized by dendrochronology to derive past annual weather dynamics from tree-ring data (Eggertsson 2019). In Figure 9, the residuals from the two annually measured plots over six years are shown. The are no obvious biases in the residuals, but there might be systematic errors in some years, when the summer has been cold, dry, etc.

The dataset for growth modelling in this study had some limitations, which made the modelling more challenging and may also affect the model prediction. The data had insufficient representation of stands older than 30 years and of dense unthinned stands. Also, some parts of Iceland are not represented in the dataset. To improve future modelling efforts, it is necessary to continue the measurement of the current permanent plots, establish new plots in areas where no data are available and leave some of the plots unthinned to provide information for mortality models. Our results pave the way for further studies on optimizing plantation management for maximal yield, carbon sequestration or economic profitability, or for just evaluating alternative management regimes for black cottonwood.

REFERENCES

Bailey RL & Dell TR 1973. Quantifying diameter distributions with the Weibull distribution. *Forest Science* 19(2), 97–104.

Barrio Anta M & Dieguez-Aranda U 2005. Site quality of pedunculate oak (*Quercus robur* L.) stands in Galicia (Northwest Spain). *European Journal of Forest Research* 124, 19-28. https://doi.org/10.1007/s10342-004-0045-3

Bogason JA, Jónsson JÁ & Sigurðsson BD 2018. Er framleiðsla iðnviðar með skammlotuskógrækt raunhæf hérlendis? Raunverulegt dæmi. [Is short rotation forestry realistic in Iceland. Real case]. *Skógræktarritið 2018* (2), 32-45. (In Icelandic).

Borders BE, Bailey RL & Ware KD 1984. Slash pine site index from a polymorphic model by joining (splining) nonpolynomial segments with an algebraic difference method. *Forest Science* 30, 411-423.

Bragason A 1995. Exotic trees in Iceland. *Icelandic Agricultural Sciences* 9, 37-45.

Burkhart HE & Tomé M 2012. *Modelling forests trees and stands*. Springer Dordrecht. 457 p. https://doi.org/10.1007/978-90-481-3170-9

Cieszewski CJ & Bella IE 1989. Polymorphic height and site index curves for lodgepole pine in Alberta. *Canadian Journal of Forest Research* 48(10), 1124-1134. https://doi.org/10.1139/x89-174

Clutter JL, Fortson JC, Pienaar LV, Brister GJ & Bailey R 1983. *Timber management: A quantitative approach*. John Wiley & Sons, New York. 333 p.

Curtis RO 1967. Height-diameter and height-diameter age equations for second-growth Douglas fir. *Forest Science* 13(4), 365–375.

Curtis RO, Clendenen GW & Demars DJ 1981. *A new stand simulator for Coast Douglas-fir: DFSIM user's guide*. U.S. Forest Service, Pacific Northwest Forest and Range Experiment Station, Portland, Oregon. Gen. Tech. Rep. PNW-128.

de-Miguel S, Guzmán G, Pukkala T 2013. A comparison of fixed- and mixed-effects modeling in tree growth and yield prediction of an indigenous neotropical species (*Centrolobium tomentosum*) in a plantation system. *Forest Ecology and Management* 291, 249-258. https://doi.org/10.1016/j.foreco.2012.11.026

de-Miguel S, Pukkala T, Morales M 2014. Using optimization to solve tree misidentification and uneven measurement interval problems in individual-tree modeling of Balsa stand dynamics. *Ecological Engineering* 69, 232-236. https://doi.org/10.1016/j.ecoleng.2014.04.008

Eggertsson Ó 2019. Vöxtur alaskaaspa (*Populus tricocarpa*) á Sandlækjarmýri – mælingar með síritandi þvermálsmælum. [Growth of black cottonwood (*Populus tricocarpa*) in Sandlækjarmýri – measurd with band dendrometer]. *Skógræktarritið 2019* (1), 34-38. (In Icelandic).

Heiðarsson L & Pukkala T 2012. Models for simulating the development of Siberian larch (*Larix sibirica* Ledeb.) plantations in Hallormsstaður Iceland. *Icelandic Agricultural Sciences* 25, 13-23.

Heiðarsson L, Pukkala T & Snorrason A 2022. Individual-tree growth models for Sitka spruce (*Picea sitchensis*) in Iceland. *Icelandic Agricultural Sciences*. 35, 3-16. https://doi.org/10.16886/IAS.2022.01

Heiðarsson L, Pukkala T & Snorrason A 2023. Individual-tree growth models for lodgepole pine (*Pinus contorta*) in Iceland. *Icelandic Agricultural Sciences* 36, 81-93. https://doi.org/10.16886/IAS.2023.07.

Heinonen T, Pukkala T, Kellomäki S, Strandman H, Asikainen A, Venäläinen A & Peltola H 2018. Effects of forest management and harvesting intensity on the timber supply from Finnish forests in a changing climate. *Canadian Journal of Forest Research* 48(10), 1124-1134. https://doi.org/10.1139/cjfr-2018-011.

Jin X, Pukkala T, Li F, Dong L 2019. Developing growth models for tree plantations using inadequate data – a case for Korean pine in Northeast China. *Silva Fennica* 53(4), 10217. https://doi.org/10.14214/sf.10217

Jóhannsdóttir 2012. Áhrif upphafsþéttleika lerkis á viðarvöxt og trjágæði. [Effect of larch planting density on production and wood quality in larch]. (BSc thesis), Agricultural university of Iceland, Hvanneyri. 55 p.

Juma R, Pukkala T, de-Miguel S & Muchiri M 2014. Evaluation of different approaches to individual tree growth and survival modelling using data collected at irregular intervals – a case for *Pinus patula* in Kenya. *Forest Ecosystems* 1, 14. https://doi.org/10.1186/s40663-014-0014-3.

Korf V 1939. A mathematical definition of stand volume growth law. *Lesnicka Prace* 18, 337–339.

McDill ME & Amateis RL 1992. Measuring forest site quality using the parameters of a dimensionally compatible height growth function. *Forest Science* 38(2), 409–429.

Mehtätalo L, de-Miguel S & Gregoire TG 2015. Modelling height-diameter curves for prediction. *Canadian Journal of Forest Research* 45, 826-837. https://doi.org/10.1139/cjfr-2015-0054

Mikaelsson, L 2011. Productivity and biomass partitioning in 20-year Black cottonwood at variable spacing. (MSc thesis), Agricultural university of Iceland, Hvanneyri. 49 p.

Monserud RA 1984. Height growth and site index curves for inland Douglas-fir based on stem analysis data and forest habitat type. *Forest Science* 30(4), 943–965. https://doi.org/10.1093/forestscience/30.4.943.

Munro D 1974. Forest growth models – a prognosis, in: Fries J. (Ed.), Growth models for tree and stand simulation, *Proceedings of the IUFRO working party S4.01-4*, pp 7–21.

Newton PF, Lei Y & Zhang SY 2005. Stand-level diameter distribution yield model for black spruce plantations. *Forest Ecology and Management* 209, 181–192. https://doi.org/10.1016/j.foreco.2005.01.020.

Näslund M 1937. Skogsförsöksanstaltens gallringsförsök i tallskog (Forest research intitute's thinning experiments in Scots pine forests). Meddelanden från statens skogsförsöksanstalt Häfte 29 (In Swedish).

Óskarsson Ú, Jónsson TH & Thórarinsson K 1990. Rapid propagation of *Populus trichocarpa* Torr. & Gray ex Hook. I. Effects of shearing of leaves and shoot tips on survival and growth of short, soft cuttings. *Icelandic Agricultural Sciences* 4, 37-40. [In Icelandic, English Summary].

Palahí M & Pukkala T 2003. Optimising the management of Scots pine (*Pinus sylvestris* L.) stands in Spain based on individual-tree models. *Annals of Forest Science* 60, 95–107. https://doi.org/10.1051/forest:2003002

Palahí M, Tomé M, Pukkala T, Trasobares A & Montero G 2004. Site index model for *Pinus sylvestris* in north-east Spain. *Forest Ecology and Management* 187(1), 35–47. https://doi.org/10.1016/S0378-1127(03)00312-8.

Posit team (2023). *RStudio: Integrated Development Environment for R. Posit Software*, PBC, Boston, MA. http://www.posit.co/. Version 2023.9.1.494

Pukkala T, Lähde E & Laiho O 2011. Using optimization for fitting individual-tree growth models for uneven-aged stands. *European Journal of Forest Research* 130(5), 829-839. https://doi.org/10.1007/s10342-010-0475-z.

Richards FJ 1959. A flexible growth function for empirical use. *Journal of Experimental Botany* 10, 290–300.

Schumacher FX 1939. A new growth curve and its application to timber yield studies. *Journal of Forestry* 37, 819−820.

Shaw JD & Packee EC 1998. Site index of balsam poplar/western black cottonwood in interior and southcentral Alaska. *Northern Journal of Applied Forestry* 15(4), 174-181.

Sigurdsson BD 2001. *Environmental control of carbon uptake and growth in* Populus trichocarpa *plantation in Iceland*. Doctoral thesis. Swedish University of Agricultural Sciences. Uppsala. 64 p.

Skovsgaard JP, Vancley JK 2008. Forest site productivity: a review of the evolution of dendrometric concepts for even-aged stands. *Forestry* 81(1), 13-31. https://doi.org/10.1093/forestry/cpm041.

Temesgen H, Monleon V.J, Hann D.W, 2008. Analysis and comparison of nonlinear tree height prediction strategies for Douglas-fir forests. *Canadian Journal of Forest Research* 38, 553-565. https://doi.org/10.1139/X07-104.

Vanclay JK 1994. Modelling forest growth and yield: applications to mixed tropical forests. Wallingford (CT): CAB International. 312 p.

Varian H 2005. Bootstrap Tutorial. Mathematica Journal 9, 768–775.

Vedurstofa Islands 2017. Accessed on 26.1.2024 at http://www.vedur.is/Medaltalstoflur-txt/Arsgildi.html.

Weiskittel AR 2014. Forest growth and yield models for intensively managed plantations. In Borges et al. (Eds) *Management of Industrial Forest Plantations*, Springer, pp 61-90. https://doi.org/10.1007/978-94-017-8899-1_3

Received 23.3.2024
Accepted 12.6.2024

www.ias.is
https://doi.org/10.16886/IAS.2024.04 ICEL. AGRIC. SCI. 37 (2024), 39-52

Studies on the relationship between live weight and body condition score and estimation of standard reference weight of ewes from the Icelandic sheep breed

Jóhannes Sveinbjörnsson and Eyjólfur K. Örnólfsson

Agricultural University of Iceland, Faculty of Agricultural Sciences, Hvanneyri, IS-311 Borgarnes, Iceland.
E-mail: jois@lbhi.is; eyjo@lbhi.is

ABSTRACT

The aim of the study was to define the mature live weight of Icelandic sheep breed ewes. Data on body condition scores (BCS) and live weight (LW) spanning 22 production years from the Hestur research farm were analyzed to fit the linear relationship LW = **a** + **b** x BCS of ewes in different age categories. Ewe live weight continued to increase until 5 years of age. A general estimate of standard reference weight (SRW) of a mature Icelandic ewe is 70.4 ± 3.4 kg, standardized at BCS 3. For mature ewes, approximately 8.5 kg LW is needed to raise BCS by one unit. SRW creates opportunities for studies relating mature weight to other important genetic traits and for analysing the independent effects of SRW, degree of maturity, and BCS on animal performance.

Keywords: mature weight, mixed model, ewe age, nutrient requirements, herd data, growth.

YFIRLIT

Rannsókn á samhengi lífþunga og holdastiga og ákvörðun staðlaðs fullorðinsþunga íslenskra áa

Markmið rannsóknarinnar var að ákvarða fullorðinsþunga íslenskra áa. Gögn um holdastig (BCS) og lífþunga (LW) sem náðu yfir 22 framleiðsluár á fjárbúinu að Hesti voru greind tölfræðilega, út frá hinu línulega samhengi LW = **a** + **b** x BCS fyrir ær á mismunandi aldursárum. Ærnar náðu að jafnaði fullum þroska á fimmta aldursári. Fullorðinsþungi (SRW) fyrir íslenskar ær, staðlaður að holdastigi 3, reyndist vera 70,4 ± 3,4 kg. Hjá fullþroskuðum íslenskum ám þarf um 8,5 kg lífþunga til að auka hold um sem nemur einu holdastigi. Greiningin skilaði einnig mati á stöðluðum fullorðinsþunga einstakra gripa í gagnasafninu. Það gefur möguleika á rannsóknum sem tengja fullorðinsþunga við aðra mikilvæga eiginleika í kynbótastarfi. Við þetta skapast einnig möguleikar á að greina aðgreind áhrif fullorðinsþunga, þroskastigs og holda á framleiðslugetu ánna.

INTRODUCTION

Growth and development of an animal and its components in relation to size (Hammond 1932, Huxley 1932) can be fitted to functions that are common across domestic mammals when scaled according to their mature body size (Brody 1945). These genetic scaling rules were first tested for sheep by McClelland et al. (1976), and it is well established that the pattern of fat and protein deposition in sheep is remarkably similar across genotypes when scaled as a proportion of mature size (Oddy & Sainz 2002). Empty body gain in very young animals can contain a protein to fat in the ratio of 2:1, whereas in an animal approaching full maturity this ratio can be 1:7. The energy content per kg fat is more than double that of protein; for each kg protein

growth approximately 3.5 kg water and ash will be added. Therefore, the energy content of gain of an almost mature animal is typically 2.5 times greater than the energy content of gain of a very young animal, but protein content is the opposite (CSIRO 1990).

An animal that has reached full maturity does not have constant live weight or fat to protein ratio in an empty body. Fat reserves decrease at times of negative energy balance, such as in late pregnancy and lactation, but increase in the easier times of the production cycle. It is important to have methods to account for this mobilization of body reserves, for key tasks such as nutrition planning. Weight changes alone are not accurate measures, due to changes in gut fill and stage of the production cycle. Body condition score is a common assessment of the amount of muscle and fat (Kenyon et al. 2014). Jefferies (1961) proposed a body condition scoring system for sheep, with grades defined according to specific anatomical features in the lumbar region, assessed by palpation. Russel et al. (1969) further adapted this system and demonstrated its superiority over live weight alone to estimate the fat content of an animal.

The frame size of mature animals differ among breeds of the same species, sexes and individuals of the same sex. While frame size is an important determinant of an animal's live weight, so is the animal's body condition. A large-framed animal in poor condition can have the same live weight as a smaller-framed animal in good condition. A concept that connects frame size, live weight and body condition is the Standard Reference Weight (SRW), which was defined for any particular breed and sex of cattle or sheep as the approximate liveweight (LW) achieved by that animal when skeletal development is complete and the empty body contains 250 g fat/kg (CSIRO 1990), corresponding to body condition score (BCS) 3.0 for sheep on the 0-5 scale described by Russel et al. (1969).

The SRW is a useful concept for several purposes: 1) to relate live weight and body condition for mature animals; 2) to define the maturity of growing animals; 3) to estimate with higher accuracy, with the animal's estimated degree of maturity, its energy and protein requirements for growth, due to more accurate estimates of the fat, protein, and energy content of the gain.

The rules of scaling growth functions, according to mature size as described above, were adapted into ruminant nutrient formulation through the concept of SRW and generalized equations (CSIRO 1990). These principles were adapted into nutrient requirement estimates for Icelandic sheep (Sveinbjörnsson & Ólafsson 1999). However, the SRW used was only a rough estimate, as is the case with much of the mature weights for different breeds, when it is used for selecting slaughter weights and estimating nutrition requirements in different countries and production systems (CSIRO 1990, AFRC 1993, NRC 2007). Among the reasons for this inaccuracy has been a lack of data and/or analysis of data that takes into account physiological principles and different production systems.

One of the issues that arises when adult weight is determined is to what level of body condition should the mature weight be standardized. This can depend on the purpose for which the determination of mature weight is intended. When the purpose is to improve lamb meat production by fulfilling nutrient requirements according to lamb growth curves derived in nutrient non-limiting environment, it seems logical to standardize adult weight at high BCS (Friggens et al. 1997, Zygoyiannis et al. 1997a & 1997b). However, when the challenges are related to the growth, development and management of ewes in extensive or semi-extensive production systems, it has been concluded that a standardized mature weight should use a BCS in the middle of the scale, at BCS 2.5 (Cannas and Boe 2003) or 3 (CSIRO 1990).

In Iceland, most ewes are mated in their first year of life, and their fertility and overall production throughout their life is high. There is, however, no clear focus on increasing ewe growth and development in dry periods in their early years. Data of actual mature weight, both

for the breed in general and, if possible, for individual animals will aid in defining more accurate nutrition and management strategies. There is a well-known positive relationship between animal metabolic live weight and maintenance requirements (CSIRO 1990, AFRC 1993, NRC 2007). Furthermore, mature size has important genetic correlations with feed intake, methane emissions, feed efficiency, carcass composition and meat quality (Rose et al. 2023). The optimal mature weight can depend on the nature of the production system.

Studies of the relationships between ewe live weights and body condition score (McHugh et al. 2019, Semakula et al. 2020 & 2021) have demonstrated the importance of using datasets, not only with a high number of animals, but also with repeated measurements on the same animal at different ages and in different stages of the annual production cycle. The effect of pregnancy on ewe live weight is too large to ignore, but data points in pregnancy need to be corrected for the estimated weight of the conceptus (McHugh et al. 2019, Semakula et al. 2021).

The aim of the current study was to define the standard reference weight at body condition score 3.0 (SRW@BCS3) for ewes of the Icelandic breed kept in a semi-extensive system: (1) for the breed in general, for use in defining nutrient requirements and (2) for individual animals in the flock under study, for use in follow-up studies.

MATERIALS AND METHODS

Animals and management

This study used data from the Agricultural University of Iceland Hestur experimental sheep farm, based in Borgarfjörður, Southwest-Iceland. The farm is managed under conditions typical for Icelandic sheep production: indoor feeding from November to May, grazing cultivated land and natural pastures surrounding the farm from May to June, extensive grazing on common mountain pastures or highland ranges from late June to mid-September, grazing cultivated or improved grassland land until housing in November. Mating takes place in December and lambing in May. Icelandic sheep breed ewes (Aðalsteinsson 1981, Dýrmundsson and Niznikowski 2010) were shorn at the onset of the indoor feeding in November, and again in early March. Transabdominal ultrasound pregnancy scanning took place in February. The winter feed was predominantly grass haylage conserved in round bales, fed ad lib. The quality of the haylage was controlled for different feeding periods as far as possible to meet feeding standards at any time (Sveinbjörnsson & Ólafsson, 1999). Haylage was supplemented with concentrate (100-300 g d^{-1} ewe^{-1}) in the last 3-6 weeks before lambing and the first week after lambing. For more details about the production system, see Sveinbjörnsson et al. (2021).

Data

The study included data from production years 2001-2022. The database included ewe and lamb records with different variables as described in Sveinbjörnsson et al. (2021). For this study ewe records with the following variables were used: ewe ID number, year of birth, year of age, lambing date, number of lambs born and number of lambs reared within each production year. Live weight (LW) and body condition score (BCS) were recorded at five week intervals from October till late April. Body condition scoring was conducted according to the 0-5 scale with 0.25 units, as described by Russel et al. (1969).

Stages of the annual cycle are defined as follows, with abbreviations and approximate dates (± 1 to 2 days) of LW and BCS measurements in parentheses: Post-weaning (Post-W, 18 October); Pre-mating (Pre-M, 1 December); Post-mating (Post-M, 4 January); 2-Month pregnant (2 Mo-preg, 10 February); Mid-pregnancy (Mid-preg, 15 March); Late-pregnancy (Late-preg, 20 April).

The estimated weight of the conceptus was calculated using the formulas reported by Robinson et al. (1977) for crosses of Finnish Landrace and Dorset Horn ewes. These breeds have a closer resemblance to the Icelandic sheep breed in gestation length, prolificacy and adult size (Robinson et al. 1977, Anderson et al. 1981,

Dýrmundsson and Ólafsson 1989) than other breeds in similar studies, e.g. the Merino sheep (Wheeler et al. 1971). Information required for the use of the formulas of Robinson et al. (1977) was available in our database, i.e., date of mating or lambing, number of foetuses and weight of the ewe at a date close to the date of mating. During pregnancy, ewe live weight was corrected for the estimated weight of the conceptus, thereby creating a new variable, pregnancy-free live weight (PFLW).

Statistical analyses

Statistical analyses were performed using SAS (2015). PROC GLM was used for simple ANOVA analysis and calculating least square means as presented in Table 1, Figure 1 and Figure 2. Simple linear regression was used for the analysis presented in Tables 2 and 3, where within year of age, pregnancy-free live weight (PFLW) was regressed against BCS for data from each year of age (Table 3) and stage of the annual cycle (Table 2). Some more complex relationships were tested, but none gave a better prediction than the simple linear relationship: PFLW = **a** + **b** x BCS. Mixed model analysis (PROC MIXED) was used for the results presented in Table 4, where PFLW was regressed against BCS for data from each year of age and the effect of an individual ewe in the dataset was considered as a random classification effect.

Definition of sub-datasets for different statistical analysis

For the analysis reported in Tables 2-7, we used a subset of the dataset, where "full" records for LW and BCS (at least 22 of 24 possible) were available for individual ewes on their 2nd to 5th year of age. The 1266 ewes in this dataset were born in the years 1999 to 2017, the lowest number in 1999 (n=31) and the highest in 2010 (n=89). Figure 1 was generated from a sub-dataset containing ewes with full records from 2 to 6 years of age (n=889). Figure 2 and Table 1 contain data from a larger group of ewes that had full records during their 5th year of age, irrespective of whether they had full records at younger age (n=1577). The additional 311 ewes included were either born before 1999 or had several missing values at younger ages. The analysis to determine Equation 1, for prediction of PFLW from BCS, ewe age and random intercept for individual ewe, was based on records of 3344 ewes. This included all ewes between 2 to 5 years of age with LW and BCS data in production years 2001-2022, but not necessarily with full records.

RESULTS

Records for ewes with live weight and BCS from 2 to 6 years of age showed a significant increase in LW at each stage of the annual cycle each year of age up to 5 years, but not between their 5th and 6th year (Figure 1). There was, however, a significant decrease in BCS at each stage of the annual cycle by each year of age up to 6 years.

For all ewes with records during their 5th year of age, LW gain was driven by the number of foetuses and the progression of pregnancy (Figure 2a). The most rapid pregnancy-free LW gain (PFLW) was observed between weaning and mating (Figure 2b). By correcting live weight for the estimated weight of the

Table 1. The ratio of PFLW/BCS at different stages of the production year for 1577 ewes at 5 years of age, dataset defined as for Figure 2.

Production stage	Barren	Single	Twin	Triplet
Post-W	23.70^{b}	23.15^{c}	23.03^{d}	23.66^{b}
Pre-M	23.43^{b}	23.11^{c}	22.62^{c}	23.39^{b}
Post-M	23.41^{b}	22.57^{b}	22.15^{b}	22.91^{a}
2 Mo-preg	23.07^{b}	22.44^{b}	22.15^{b}	22.87^{a}
Mid-preg	21.68^{a}	21.64^{a}	21.50^{a}	22.75^{a}
Late-preg	21.38^{a}	22.70^{b}	22.47^{c}	23.75^{b}
N	41	206	1118	212
SEM	0.47	0.25	0.13	0.22

a, b, c: Values with different superscripts within a column are statistically different, $p<0.05$.

SEM: standard error of the means

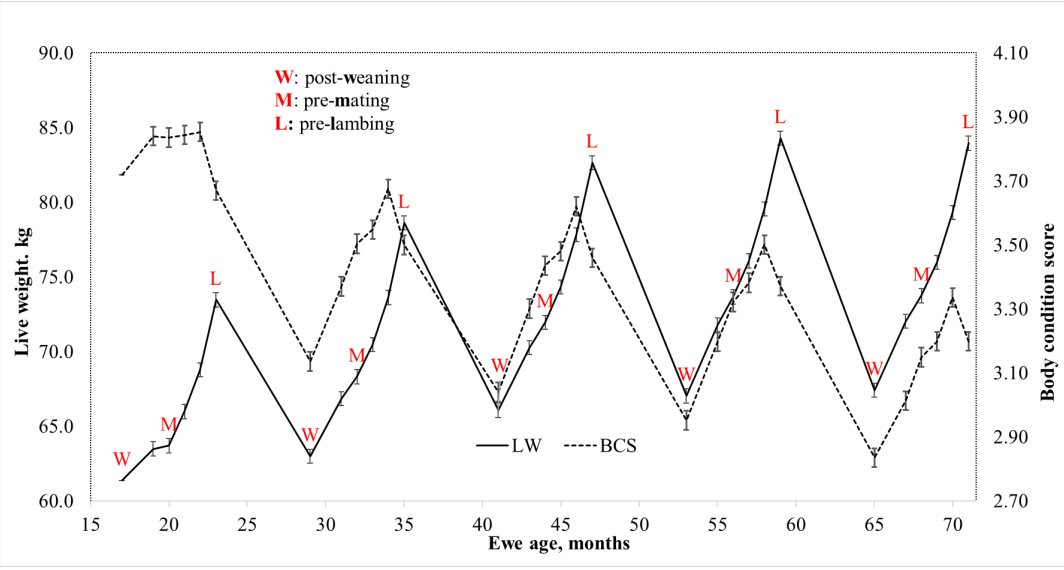

Figure 1. Ewe live weight (LW) and body condition score (BCS) of 889 ewes between 18 months and six years of age at post-weaning (W), pre-mating (M) and pre-lambing (L). Error bars indicate 95% confidence interwals.

conceptus, the weight differences related to litter size disappeared for single and twin ewes, but the triplet-bearing ewes were still heavier troughout the production cycle.

For all litter sizes, BCS (Figure 2c) increased from weaning to mating but then increased at a slower rate with progressing pregnancy. Immediately before mating (Pre-M), ewe BCS was similar among litter size classes. After mating, BCS increased for all litter sizes, until it decreased in Late-preg for twin- and triplet-bearing ewes. The ratio PFLW/BCS was highest in autumn (Table 1). Among twin-bearing ewes, the ratio decreased steadily through winter until increasing again between Mid-preg and Late-preg. There was a similar trend for single- and triplet-bearing ewes but with fewer statistical differences, due to smaller group sizes. In periods when BCS was increasing, the ratio PFLW/BCS decreased, and vice versa. This pattern was seen among barren ewes, which gained the same amount of condition (Figure 2c) from weaning (Post-W) to mating (Pre-M) as the other groups, but less BCS in the first half of the pregnancy period and more in the latter half, with a decrease in the ratio PFLW/BCS (Table 1).

The regression coefficients for the simple linear relationship PFLW = **a** + **b** x BCS for each year of age and production stage are reported in Table 2 and compared statistically, according to 95% confidence limits. The constant **a** generally had a lower value and the slope **b** higher value for 2-year-old ewes than for other age categories in the different stages of the production cycle. By using the prediction equations derived by the regressions, LW at BCS=3 was calculated for each age category and production stage (Table 2). Similarly, Table 3 reports the linear regression coefficients within each year of age, with all production stages combined. Here, the constant **a** increased significantly with increasing age, but the slope **b** was stable irrespective of age.

In the mixed model analysis presented in Table 4, a random intercept for the effect of individual animals in the dataset is included. The random effect of ewe was not separated between intercept and slope, therefore all the individual differences were collected in the random intercepts, which add up to zero for all animals within each year of age. The prediction error (RMSE) of the regression models generated by the mixed model analysis

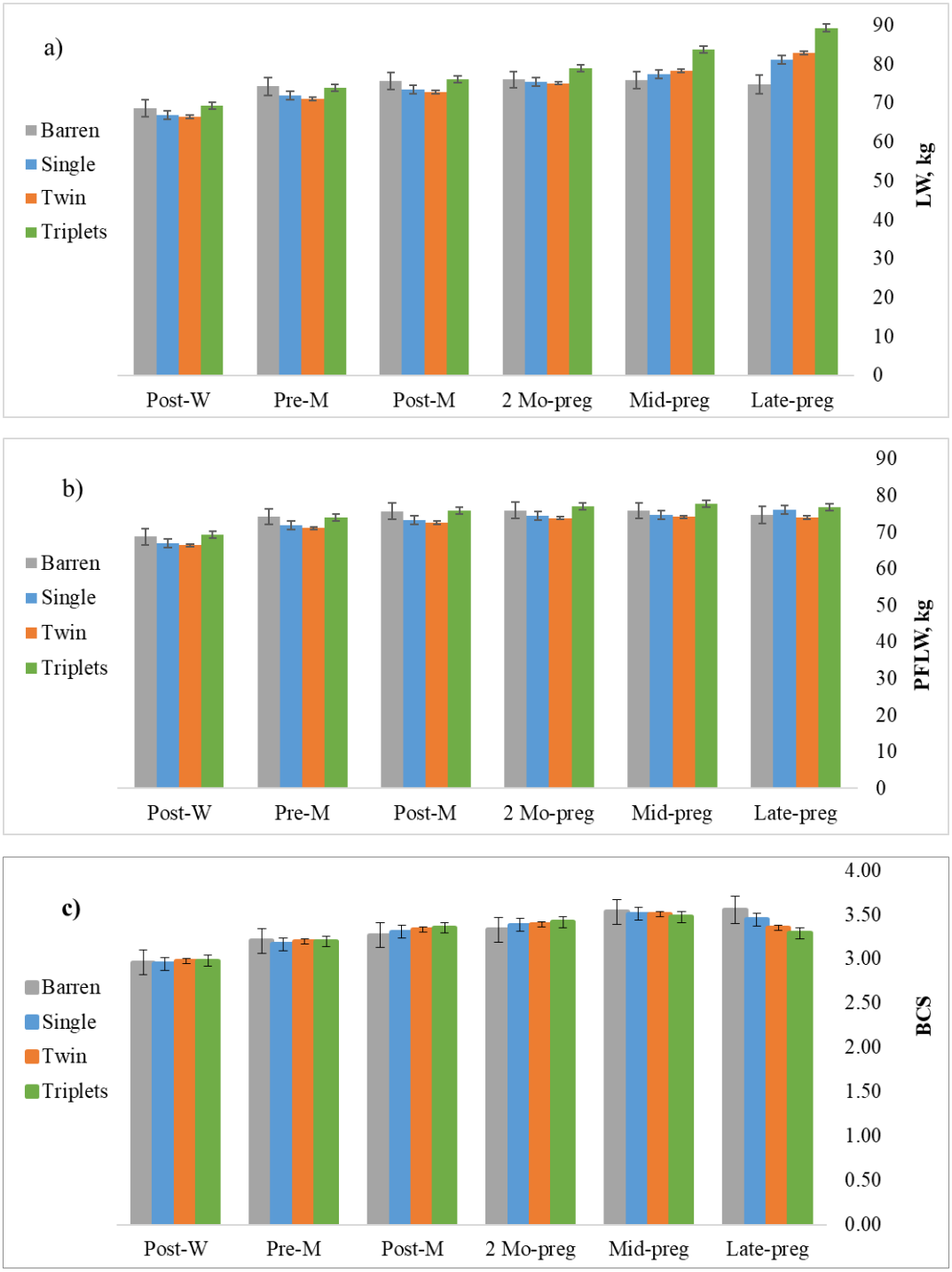

Figure 2. a) Ewe live weight (LW), b) pregnancy-free LW (PFLW) and c) body condition scores (BCS) of 1577 ewes (212 with triplets, 1118 with twins, 206 with single lamb and 41 barren) at 5 years of age. All ewes in the database with LW ands BCS records on their 5th year were included in this analysis, except for 11 ewes with quadruplets. Error bars indicate 95% confidence interwals.

Table 2. Coefficients **a** and **b** for the regressions PFLW= **a** + **b** x BCS within each year and months of age and stage of the production cycle, for 1266 ewes with at least 22 of 24 possible records of LW and BCS between their 2 to 5 years of age.

Production stage	year no	age mo	a	b	R^2	PFLW at BCS 3.00
Post-W	2	17	28.1^{a}	8.93^{B}	0.41	54.9
Pre-M	2	19	31.7^{ab}	8.33^{B}	0.35	56.7
Post-M	2	20	30.4^{ab}	8.62^{B}	0.36	56.3
2 Mo-preg	2	21	32.9^{b}	8.27^{B}	0.35	57.7
Mid-preg	2	22	29.6^{ab}	9.18^{B}	0.37	57.1
Late-preg	2	23	34.3^{b}	8.47^{B}	0.30	59.7
Post-W	3	29	42.6^{c}	6.46^{A}	0.23	62.0
Pre-M	3	31	42.9^{cd}	7.09^{AB}	0.22	64.2
Post-M	3	32	43.2^{cd}	7.12^{AB}	0.21	64.6
2 Mo-preg	3	33	41.7^{c}	7.79^{AB}	0.25	65.1
Mid-preg	3	34	37.0^{bc}	8.91^{B}	0.28	63.8
Late-preg	3	35	37.3^{bc}	9.41^{B}	0.29	65.5
Post-W	4	41	45.7^{cd}	6.61^{AB}	0.22	65.5
Pre-M	4	43	47.8^{d}	6.93^{AB}	0.19	68.6
Post-M	4	44	47.9^{d}	6.95^{AB}	0.20	68.8
2 Mo-preg	4	45	46.6^{cd}	7.64^{AB}	0.24	69.5
Mid-preg	4	46	41.1^{c}	8.97^{B}	0.27	68.1
Late-preg	4	47	44.6^{cd}	8.43^{B}	0.24	69.9
Post-W	5	53	47.7^{d}	6.57^{A}	0.21	67.4
Pre-M	5	55	48.5^{d}	7.31^{AB}	0.19	70.5
Post-M	5	56	50.4^{d}	6.92^{AB}	0.18	71.1
2 Mo-preg	5	57	47.4^{d}	8.07^{B}	0.24	71.6
Mid-preg	5	58	44.1^{cd}	8.88^{B}	0.27	70.7
Late-preg	5	59	43.3^{cd}	9.42^{B}	0.29	71.5

$^{a, b, c}$ or $^{A, B, C}$: Values with different superscripts within a column are statistically different, $p<0.05$. PFLW = pregnancy-free live weight

(Table 4) was approximately half of those from the linear model (Table 3). Here, the slope **b** increases with increasing age of the ewes. There was a good agreement between the linear (Table 3) and mixed (Table 4) model analysis in estimated LW at different BCS, according to the regression equations, especially with increasing age.

By using all records for ewes with some, but not necessarily all, LW and BCS data between 2 to 5 years of age in production years 2001-2022, Equation 1 was derived:

Eq. 1: $PFLW=R_{ewe} + 19.52(0.215)+7.95(0.039)\cdot BCS+8.72(0.051)\cdot year-0.64(0.006)\cdot year^2$

where R_{ewe} is the random intercept for individual ewe and year is the ewe‘s year of age. The values in parentheses are the standard errors for the respective regression coefficients, the prediction error (RMSE) for the whole equation is 3.67 kg. A total of 3344 ewes were included in this analysis.

Predictions of LW at BCS=3 for individual animals at specific ages based on the mixed

Table 3. Coefficients **a** and **b** for linear regressions PFLW= **a** + **b** x BCS within each year of age, combined for the six stages of the production cycle, for 1266 ewes with at least 22 of 24 possible records of LW and BCS between 2 to 5 years of age. Predicted LW at different BCS as calculated from the respective regression equations.

			LW at BCS:			
Year	**a** (SE)	**b** (SE)	2.00	3.00	4.00	RMSE
2	31.6^{a} (0.53)	8.51^{A} (0.139)	48.6	57.1	65.7	5.8
3	38.2^{b} (0.53)	8.59^{A} (0.153)	55.4	64.0	72.5	6.1
4	42.2^{c} (0.53)	8.66^{A} (0.156)	59.5	68.1	76.8	6.4
5	43.6^{c} (0.53)	8.90^{A} (0.162)	61.4	70.3	79.2	6.8

$^{a, b, c}$ or $^{A, B, C}$: Values with different superscripts within a column are statistically different, $p<0.05$.

RMSE = root-mean-squared error

Table 4. Coefficients **a** and **b for** PFLW= **a** + **b** x BCS for mixed model regressions including random intercept for the effect of individual animals; within each year of age, combined for the six stages of the production cycle, for 1266 ewes with at least 22 of 24 possible records of LW and BCS between 2 to 5 years of age. Predicted LW at different BCS as calculated from the respective regression equations.

			LW at BCS:			
Year	**a** (SE)	**b** (SE)	2.00	3.00	4.00	RMSE
2	43.6^{bc} (0.53)	5.37^{A} (0.134)	54.3	59.7	65.0	2.8
3	40.2^{a} (0.45)	8.00^{B} (0.123)	56.2	64.2	72.3	3.1
4	42.7^{b} (0.45)	8.49^{C} (0.124)	59.7	68.2	76.6	3.2
5	44.7^{c} (0.45)	8.56^{C} (0.130)	61.9	70.4	79.0	3.4

$^{a, b, c}$ or $^{A, B, C}$: Values with different superscripts within a column are statistically different, $p<0.05$.

RMSE = root-mean-squared error

Table 5. Comparison of two different estimates of LW at BCS=3 for individual animals at various ages by linear regressions Y= **a** + **b** x X. The dependent variable Y is the value estimated by eq. 1 and the independent variable X is the value estimated by the regressions in Table 4.

Year	**a** (SE)	**b** (SE)	R^2	RMSE
2	5.1^{a} (0.77)	0.89^{ab} (0.013)	0.79	2.34
3	3.9^{a} (0.66)	0.93^{b} (0.010)	0.87	1.86
4	6.6^{a} (0.63)	0.90^{b} (0.009)	0.88	1.75
5	10.9^{b} (0.59)	0.85^{a} (0.008)	0.89	1.68

$^{a, b, c}$: Values with different superscripts within a column are statistically different, $p<0.05$.

RMSE = root-mean-squared error

model analysis in Table 4 were then compared to predictions of LW at BCS=3 for the same 1266 ewes at specific ages by Equation 1. As reported in Table 5, the agreement between the two methods is good, although poorer for ewes in their 2nd year than for the older ewes.

Some of the variation in the development of LW adjusted to BCS=3 in 2nd to 5th year, as reported in Tables 3 and 4, can be related to birth years and whether the ewes did or did not rear lambs in their 1st year (Table 6).

There is a considerable distribution in mature weights (SRW@BCS3) of individual animals (Table 7), slightly greater when estimated by the mixed model than by Equation 1.

Table 6. LW at BCS=3 reached in 2nd, 3rd and 4th year of age as a proportion of LW at BCS=3 at 5th year of age, depending on whether ewes reared 0 or 1 lamb in their 1st year of age. Average, max and min values for birth years 1999 to 2017.

Rearing in 1st year	2nd year		3rd year		4th year	
	0	1	0	1	0	1
Average	0.87	0.84	0.92	0.91	0.97	0.97
max	0.90	0.87	0.97	0.96	1.01	1.01
min	0.81	0.78	0.84	0.82	0.92	0.92

Table 7. Estimated standard reference weight (SRW@BCS3) for 1266 ewes, by the mixed model (Table 5) and Equation 1, frequency in different weight (SRW) categories.

SRW, kg	Mixed model	Equation 1
≤60.0	2.9%	0.6%
60.1-65.0	15.1%	12.5%
65.1-68.0	15.7%	16.7%
68.1-72.0	28.4%	29.9%
72.1-75.0	16.9%	19.0%
75.1-80.0	15.4%	16.9%
≥80.1	5.6%	4.4%

DISCUSSION

The main purpose of this study is to define the mature weight, or more exactly the standard reference weight (SRW), at body condition score 3 (SRW@BCS3) of ewes of the Icelandic sheep breed, for a more exact determination of energy and protein requirements. Our study was inspired by earlier work, such as Zygoyiannis et al. (1997b) who proposed a method to estimate mature weight of different breeds of sheep by accounting for data on ewe age and body condition, as well as live weight records, which was analyzed to fit the linear relationship LW = **a** + **b** x BCS for ewes in different age categories. The mature weight is then found as LW calculated from this formula based on a certain BCS and **a** and **b** coefficients found for an age group that has reached maturity. Estimating the **b** slope in the regression formula accurately is particularly important, as it expresses how many kg LW can be expected to follow each unit of BCS. If this is known, each BCS mobilized or deposited through the annual production cycle can be translated into energy, which is very important in feed planning. This has been the focus of many studies on the relationships between live weights and body condition scores in ewes, e.g. Cannas and Boe (2003), Macé et al. (2019); McHugh et al. (2019) and Semakula et al. (2020).

An important question in this context is: when is full maturity achieved? Zygoyiannis et al. (1997b) analyzed data for ewes of three Greek breeds and assumed that full maturity was reached at 3.5 years of age, since with higher ages there was no significant increase in LW adjusted to a certain level of BCS. In the current study, analysis of ewes with complete records up to 6 years of age (Figure 1) found that, although the ewes did not gain weight after their 5th year, they continued to loose condition. LW adjusted to BCS 3 increased significantly from 5th to 6th year, although this was due to lower BCS at the 6th year, not a higher LW. Therefore, it was assumed that full maturity was reached at 5 years of age, and all subsequent analysis were based on that assumption. Available evidence suggested that the Icelandic sheep breed

deposits relatively more fat internally and less fat in carcass than the more specialized mutton breeds and particularly deposits a low proportion of subcutaneous fat relative to the rest of the fatty tissue, which was more pronounced with increasing age (Thorgeirsson & Thorsteinsson, 1989).

Live weight in pregnancy was corrected for the estimated weight of the conceptus, as per McHugh et al. (2019) and Semakula et al. (2021). Using the pregnancy-free live weight (PFLW) allowed for additional LW and BCS during pregnancy to be used to increase data points from three to six per year. For the analysis to define the average SRW@BCS3 for ewes of the Icelandic sheep breed, records for 1266 ewes were used. Although other studies have used repeated measurements on the same ewes, to our knowledge no studies have utilized only complete records for the same animals over many years of age. This created an opportunity to isolate individual variation from the residual error. The results presented in Table 4 allow us to define the SRW@BCS3 for ewes of the Icelandic sheep breed as 70.4 ± 3.4 kg. Each unit of BCS for mature Icelandic ewes was approximately 8.5 kg LW.

Adult weight of three Greek breeds was estimated to be 41.6, 52.3 and 61.4 kg when standardized at condition score 3 and 56.3, 69.8 and 80.0 at condition score 5, for the Boutsko, Serres and Karagouniko breeds, respectively (Zygoyiannis et al. 1997b), using a similar method as our study. The SRW@BCS3 for female sheep of breeds of different sizes in Australia according to CSIRO (1990) was between 40-60 kg. These estimates were low compared to mature sizes of ewes of common breeds in the UK (AFRC 1993) and USA (NRC 2007). Icelandic sheep would be classified as medium-sized breed according to our estimate of approximately 70 kg for the mature weight of ewes. The lack of systematic determination of adult weight of different sheep breeds, however, makes it difficult to compare breeds with respect to adult weight. The method used in our study is applicable for different breeds, as it is based on physiological principles that translate into nutrient requirements and feed planning. The statistical relationships that are utilized are simple and reproducible. The completeness of the dataset is important but should not be difficult to attain with modern techniques.

As seen in the three Greek breeds (Zygoyiannis et al. 1997b), the choice of level of body condition at which the mature live weight is standardized is critical and should be a part of the information reported. For mature sheep of different breeds, it would be most efficient to report both **a** and **b** coefficients for the simple linear relationship LW = **a** + **b** x BCS, assuming the relationship between LW and BCS is linear. Most studies reviewed by Kenyon et al. (2014) found this to be the case. An exception was a study by Teixeira et al. (1989) where among 52 animals, evenly distributed over the BCS scale from 1.25 to 4.50, there were greater increases in LW required to gain one BCS unit at the higher end of the BCS scale. They also demonstrated that total body fat increased at a greater rate at the higher end of the BCS scale, which was later also found by Morel et al. (2016). However, when the method of body condition scoring was originally established for sheep, a linearity of the ratio of body fat to BCS and LW to BCS was reported (Russel et al. 1969), for 276 ewes between BCS 1.00 and 3.5. Based on available information, it seems safe to assume that the relationship between LW and BCS is linear in the practical ranges of BCS, most often worked with in sheep management and feed planning. However, although the repeatability of the BCS technique by experienced assessors is good (Kenyon et al. 2014), it should always be kept in mind that it is a subjective method.

Experiments reviewed by Kenyon et al. (2014), as well as later studies by McHugh et al. (2019) and Semakula et al. (2020), showed considerable differences in kg LW required to increase BCS by one unit, although most results were between 5 and 10 kg, with differences between sexes, sheep breeds, and individuals within the same breed and sex. These differences may be due to variation in body frame size, SRW and fat distribution throughout the body. Kenyon et al. (2014) reported that most studies on the

relationship between LW and BCS were based on between-animal variation. Controlled studies investigating the relationship between LW and BCS frequently involved dissection of animals to determine body tissue composition (Russel et al. 1969, Teixeira et al. 1989, Morel et al. 2016), resulting in limited opportunity to analyze the within-animal relationship using repeated measures. For this purpose, it is possible to carry out studies where fully mature animals would be fed to create within-animal variability in LW and BCS. A more practical method is to use herd-databases with repeated measures of pregnancy-free live weight on the same animals, as in our study and that of McHugh et al. (2019). In both studies, there were considerable differences in the estimated slope (**b** coefficient), depending on stage of the production cycle (Table 2). A more robust estimate was achieved in our study when data was combined for different stages of the production cycle (Table 3) and with lower prediction error if the individual variation was isolated (Table 4).

Our estimate of the slope **b**, (8.56 kg, Table 4), or the kg LW change per unit BCS in mature Icelandic ewes, is in the higher range compared to estimates for other breeds. The estimate would have been lower (6.57-7.31; Table 2) if only some of the regressions for periods outside pregnancy for the mature ewes (5^{th} year) were used. The estimate of the slope **b** for ewes on their 5^{th} year differed slightly (8.56 vs 8.90; Tables 4 vs 3) if the individual variation was isolated using a mixed rather than linear regression analysis. The same applies to the final estimate of the SRW@BCS3, which was similar using both methods, but using the mixed model lowered the prediction error by approximately half. For the youngest and least mature (2^{nd} year) ewes, the linear model predicts similar slopes (**b**) as for older ewes, but the mixed model had lower predictions for younger ewes, which makes more sense. For future studies with similar aims, this is worth consideration.

The estimated slope **b** (8.56 kg) divided by the SRW@BCS3 (70.4 kg; Table 4) yielded the ratio 0.122, which was similar to the general ratio reported for diverse breeds of sheep (0.129) or sheep and cattle (0.1285) by Zygoyiannis et al. (1997b). For Churra ewes, Frutos et al. (1997) reported a ratio of 0.13. However, van Burgel et al. (2011) reported that Merino ewes had a 9.2 kg LW change per unit BCS, which was 0.19 times the SRW. The ewes in that study were in late pregnancy, and their live weights were not corrected for the weight of the conceptus, which could partly explain the high values.

The between-animal differences in mature weight are interesting, not only for improving the accuracy of estimates of SRW and LW per BCS for a breed in general, but also with respect to breeding targets. Larger animals have higher maintenance requirements, but also higher feed intake, which might override the increased maintenance requirements with respect to producivity and feed efficiency (Cannas et al. 2019). According to the physiological principles and genetic scaling rules addressed in the introduction, individuals with high mature weight should be leaner and have a lower degree of maturity at a certain LW, compared to animals with lower mature weight. Among Icelandic sheep, there has been a considerable genetic trend towards lower fat grade in carcasses (Eiríksson and Sigurðsson, 2017), meaning that carcasses can be heavier at the same fat grade. By breeding for leaner carcasses, it would be logical to assume that there will also be a genetic trend towards higher mature live weights. By estimating the mature weight of individual animals as in our study, it will be possible to calculate genetic correlations between mature weight and other important traits, based on data from Hestur farm.

Previously, multilevel models were used to analyze the effects of different explanatory variables, including ewe age, LW and BCS, on lamb birth weights and growth rates from Hestur farm data (Sveinbjörnsson et al. 2021). These three explanatory variables are partly related, as can be seen from the results presented in our study (Table 4). At a younger age, live weights are lower and fewer kg LW are required to increase BCS by one unit. From the analysis presented in Table 4, also accounting for the random intercept for individual ewes, it

is possible to define the LW at BCS 3 of each animal in each year of age. Dividing that value with the LW at BCS 3 in the 5th year of age (Table 6), we can determine the animal's estimated degree of maturity at each year of age. This allows the analysis of the independent effects of individual SRW, degree of maturity, and BCS at particular stages in the production cycle and changes in BCS on production parameters such as ewe fertility, lamb birth weight and growth rates. For these types of studies, it seems logical to use data only for ewes that have full records until their 5th year of age. For studies of genetic parameters, it might be possible to also use data for ewes that do not have full records, by means of relationships like the one presented by Equation 1 above. The distribution in mature weights (SRW@BCS3) of individual animals was considerable in our study (Table 7), indicating possibilities for including that trait in a breeding program.

CONCLUSIONS

The standard reference weight (SRW) for ewes was estimated to be 70.4 ± 3.4 kg, for the Icelandic sheep breed. For a fully mature ewe, approximately 8.5 kg live weight was needed to raise body condition score by one unit. SRWs for individual animals were also determined, which creates opportunities for follow-up genetic and management studies.

AKNOWLEDGEMENTS

Financial support for this project from the Icelandic Sheep Productivity Fund is acknowledged. We are also grateful to all the staff at Hestur sheep farm who through the years have contributed to very comprehensive sheep production records.

REFERENCES

Aðalsteinsson S 1981. Origin and conservation of farm animal populations in Iceland. *Journal of Animal Breeding and Genetics* 98, 258-264.

AFRC 1993. *Energy and protein requirements of ruminants*. An advisory manual prepared by the AFRC technical committee on responses to nutrients. CAB International, Wallingford, UK, 159 p.

Anderson GB, Bradford GE & Cupps PT 1981. Length of Gestation in Ewes Carrying Lambs of 2 Different Breeds. *Theriogenology* 16, 119-129. https://doi.org/10.1016/0093-691X(81)90120-5

Brody S 1945. *Bioenergetics and growth*. Reinholds, New York, 1023 p.

Cannas A & Boe F 2003. Prediction of the relationship between body weight and body condition score in sheep. *Italian Journal of Animal Science* 2, 527-529. https://doi.org/10.4081/ijas.2003.s1.527

Cannas A, Tedeschi LO, Atzori AS & Lunesu MF 2019. How can nutrition models increase the production efficiency of sheep and goat operations? *Animal Frontiers* 9, 33-44. https://doi.org/10.1093/af/vfz005

CSIRO 1990. Australian Agricultural Council: *Feeding Standards for Australian Livestock: Ruminants.* INUFSL Working Party, Ruminants Subcommittee. CSIRO, Australia, 266 p.

Dýrmundsson ÓR & Niznikowski R 2010. North European short-tailed breeds of sheep: a review. *Animal* 4, 1275-1282. https://doi.org/10.1017/S175173110999156x

Dýrmundsson ÓR & Ólafsson T 1989. Sexual development, reproductive performance, artificial insemination and controlled breeding. Pages 95-104 in: Dýrmundsson ÓR & Thorgeirsson S (eds.): *Reproduction, growth and nutrition in sheep*. Dr. Halldór Pálsson Memorial Publication, Agricultural Research Institute and Agricultural Society, Reykjavík.

Eiríksson JH & Sigurðsson Á 2017. Sources of bias, genetic trend and changes in genetic correlation in carcass and ultrasound traits in the Icelandic sheep population. *Icelandic Agricultural Sciences* 30, 3-12. https://doi.org/10.16886/Ias.2017.01

Friggens NC, Shanks M, Kyriazakis I, Oldham JD & McClelland TH 1997. The growth and development of nine European sheep breeds. 1. British breeds: Scottish Blackface, Welsh Mountain and Shetland. *Animal Science* 65, 409-426. https://doi.org/10.1017/S1357729800008614

Frutos P, Mantecon AR & Giraldez FJ 1997. Relationship of body condition score and live weight with body composition in mature Churra ewes. *Animal Science* 64, 447-452. https://doi.org/10.1017/S1357729800016052

Hammond J 1932. *Growth and development of mutton qualities in the sheep*. Oliver and Boyd, Edinburgh, 597p.

Huxley J 1932. *Problems of relative growth*. Methuen, London, 276 p.

Jefferies BC 1961. Body condition scoring and its use in management. *Tasmanian Journal of Agriculture* 32, 19-21.

Kenyon PR, Maloney SK & Blache D 2014. Review of sheep body condition score in relation to production characteristics. *New Zealand Journal of Agricultural Research* 57, 38-64. https://doi.org/10.1080/00288233.2013.857698

Macé T, González-García E, Carrière F, Douls S, Foulquié D, Robert-Granié C & Hazard D 2019. Intra-flock variability in the body reserve dynamics of meat sheep by analyzing BW and body condition score variations over multiple production cycles. *Animal* 13, 1986-1998. https://doi.org/10.1017/S175173111800352X

McClelland TH, Bonaiti B & Taylor SCS 1976. Breed Differences in Body-Composition of Equally Mature Sheep. *Animal Production* 23, 281-293. https://doi.org/10.1017/S0003356100031408

McHugh N, McGovern F, Creighton P, Pabiou T, McDermott K, Wall E & Berry DP, 2019. Mean difference in live-weight per incremental difference in body condition score estimated in multiple sheep breeds and crossbreds. *Animal* 13, 549-553. https://doi.org/10.1017/S1751731118002148

Morel PCH, Schreurs NM, Corner-Thomas RA, Greer AW, Jenkinson CMC, Ridler AL & Kenyon PR 2016. Live weight and body composition associated with an increase in body condition score of mature ewes and the relationship to dietary energy requirements. *Small Ruminant Research* 143, 8-14. https://doi.org/10.1016/j.smallrumres.2016.08.014

NRC 2007. *Nutrient requirements of small ruminants: sheep, goats, cervids and new world camelids.* Committee on Nutrient Requirements of Small Ruminants. The National Academies Press, Washington, D.C., 346 p.

Oddy VH & Sainz RD 2002. Nutrition for sheep meat production. Ch. 11 (pp. 237-262) in: Freer M & Dove H (eds.): *Sheep Nutrition*. CABI Publishing, Wallingford, UK.

Robinson JJ, McDonald I, Fraser C & Crofts RMJ 1977. Studies on Reproduction in Prolific Ewes. 1. Growth of Products of Conception. *Journal of Agricultural Science* 88, 539-552. https://doi.org/10.1017/S0021859600037229

Rose G, Paganoni B, Macleay C, Jones C, Brown DJ, Kearney G, Ferguson MB, Clarke BE & Thompson AN 2023. Methane, growth and carcase considerations when breeding for more efficient Merino sheep production. *Animal* 17, 1-8 https://doi.org/10.1016/j.animal.2023.100999

Russel AJF, Doney JM & Gunn RG 1969. Subjective assessment of body fat in live sheep. *Journal of Agricultural Science*, *Cambridge* 72, 451-454. https://doi.org/10.1017/S0021859600024874

SAS 2015. SAS Enterprise Guide 7.11, ©2015. SAS Institute Inc., Cary, NC, USA (2015)

Semakula J, Corner-Thomas RA, Morris ST, Blair HT & Kenyon PR 2020. The Effect of age, stage of the annual production cycle and pregnancy-rank on the relationship between liveweight and body condition score in extensively managed Romney ewes. *Animals* 10, 784-802. https://doi.org/10.3390/ani10050784

Semakula J, Corner-Thomas RA, Morris ST, Blair HT & Kenyon PR 2021. Predicting ewe body condition score using adjusted liveweight for conceptus and fleece weight, height at withers, and previous body condition score record. *Translational Animal Science* 5, 1-12. https://doi.org/10.1093/tas/txab130

Sveinbjörnsson J, Eythórsdóttir E, Örnólfsson EK 2021. Factors affecting birth weight and pre-weaning growth rate of lambs from the Icelandic sheep breed. *Small Ruminant Research* 201,106420 https://doi.org/10.1016/j.smallrumres.2021.106420

Sveinbjörnsson J & Ólafsson BL 1999. Orkuþarfir sauðfjár og nautgripa í vexti með hliðsjón af

mjólkurfóðureiningakerfi.[Energy requirements of sheep and growing cattle with respect to milk feed unit system]. *Ráðunautafundur* 1999, 204-217. [In Icelandic].

Teixeira A, Delfa R & Colomerrocher F 1989. Relationships between Fat Depots and Body Condition Score or Tail Fatness in the Rasa Aragonesa Breed. *Animal Production* 49, 275-280. https://doi.org/10.1017/S0003356100032402

Thorgeirsson S & Thorsteinsson SS 1989. Growth, development and carcass charachteristics. Pages 169-204 in: Dýrmundsson ÓR & Thorgeirsson S (eds.): *Reproduction, growth and nutrition in sheep*. Dr. Halldór Pálsson Memorial Publication, Agricultural Research Institute and Agricultural Society, Reykjavík.

van Burgel AJ, Oldham CM, Behrendt R, Curnow M, Gordon DJ & Thompson AN 2011. The merit of condition score and fat score as alternatives to liveweight for managing the nutrition of ewes. *Animal Production Science* 51, 834-841. https://doi.org/10.1071/An09146

Wheeler JL, Reardon TF, Hedges DA & Rocks RL 1971. Contribution of conceptus to weight change in pregnant Merino ewes at pasture. *Journal of Agricultural Science*, *Cambridge* 76, 347-353. https://doi.org/10.1017/S0021859600069264

Zygoyiannis D, Kyriazakis I, Stamataris C, Friggens NC & Katsaounis N 1997a. The growth and development of nine European sheep breeds. 2. Greek breeds: Boutsko, Serres and Karagouniko. *Animal Science* 65, 427-440. https://doi.org/10.1017/S1357729800008626

Zygoyiannis D, Stamataris C, Friggens NC, Doney JM & Emmans GC 1997b. Estimation of the mature weight of three breeds of Greek sheep using condition scoring corrected for the effect of age. *Animal Science* 64, 147-153. https://doi.org/10.1017/S1357729800015654

Received 25.9.2024
Accepted 27.11.2024

Instructions to authors
(See a complete version on the website www.ias.is)

Icelandic Agricultural Sciences (Icel. Agric. Sci.) is published annually, or more frequently. The journal is in English and is refereed and distributed internationally. It publishes original articles and reviews written by researchers throughout the world on any aspect of applied life sciences that are relevant under boreal, alpine, arctic or subarctic conditions. Relevant subjects include e.g. any kind of environmental research, farming, breeding and diseases of plants and animals, hunting and fisheries, forestry, soil conservation, ecology of managed and natural ecosystems, geothermal ecology, etc.

Authors submitting a paper do so on the understanding that the work has not been published before, is not considered for publication elsewhere and has been read and approved by all authors.

Original research articles must cover new and original research that has not been published before in a medium with peer reviewing and should generally not exceed 12 printed pages, or ca. 5.000 words + tables and figures. **Short communications** focus on studies with more limited coverage than original articles. The maximum length is 4 printed pages, or ca. 2000 words. Short communications do not need an abstract. **Review articles** should generally not exceed 15 printed pages or ca. 7.000 words + tables and figures. **Letters to the Editor** are reserved for comments on articles published in IAS. They should not exceed one printed page or ca. 450 words.

Publication charges. Original articles or review articles not exceeding 12 or 15 printed pages, respectively, are free of charge. For additional pages the authors will be charged 100 € per each additional page. Supplements that may be provided with an article shall be made available on our homepage and will be charged 50€ per page.

Manuscripts should be in correct English; typed, with 1.5 line spacing on A4 paper and consisting of:

Title which should be concise and informative but as short as possible. Include also a short running title at the top of the first page.

Authors' names and name(s) and addresses of department(s)/institution(s) to which the work is attributed. Include the e-mail addresses of all authors.

Abstract, English and Icelandic "Yfirlit", should not exceed 150 words each. Non-Icelandic speaking authors will get help from the editor with translation to "Yfirlit".

Keywords in alphabetical order, up to 6 words, preferably not used in the title.

Text should normally be divided into: Introduction, Materials and methods, Results, Discussion, Acknowledgements, and References. Use capitals in first headings, use italic in second headings (and title of Icelandic "Yfirlit") and use bold and italic in third headings, if needed.

Introduction should provide a general orientation of the subject and present reasons for and aims of the study. Concisely written. Text references should be written: Smith & Jones (1988) or Hansson et al. (1990). If more than two publications are used references should be cited chronologically (Smith & Jones 1988, Hansson et al. 1990). Do not italicizes et al.

Materials and methods must provide sufficient information to permit exact replication of experimental work or statistical analysis.

Results should be clear, concise, and as objective as possible. No discussion of the results is permitted in this section.

Discussion should not repeat results, but in a logical way interpret the main results with reference to relevant figures, tables and references. The Discussion should be concisely written and as brief as possible. A separate chapter of Conclusions may be used.

Abbreviations, numberical symbols and style.

1. Use only international standard abbreviations, according to the guidelines from Caltec Library Service (http://library.caltech.edu/reference/abbreviations/).
2. In decimals, use the decimal point, not the comma (use comma in Icelandic "Yfirlit").
3. When presenting units, do not use slash (t/ha year), use negative exponents (t DM ha^{-1} $year^{-1}$). DM = dry mass.
4. When presenting concentrations, quantitative units (e.g. mg N g^{-1} DM) are preferred to relative units (e.g. % N).
5. Use no Roman numerals.
6. Foreign words, Latin names of genera, species, mathematical symbols, etc. should be italicized. Personal names after Latin names should not be italicized.
7. Indicate the Latin binomial and authority names of species when they are first mentioned in the text, but not in the title or the abstract.

References should be kept to a pertinent minimum. Primary publications in English are recommended. In the text, references are identified by the name(s) of the author(s) with the year of publication in parenthesis. If both are in parenthesis, no punctuation separates the name(s) of the author(s) and the year of publication. Consecutive citations in the text are placed in chronological order and separated by commas. If there are two authors the names are separated with the symbol &. If there are more than two authors, only the first author's name is given, and this is followed by the phrase et al., which should not be in italic (e.g. Kramer 1986, Day et al. 2002). In the reference list names of journals should be written out fully. The reference list should be arranged in alphabetical order according to the name of the first author, see examples below. Titles of articles in other languages than English, French or German should be translated to English, in brackets, and the language of the original source should be indicated in brackets at the end of the reference. Names of authors and publication year should be in bold, separating authors with commas but apart from that without commas or dots. Name of journal or books should be italicized.

DOI numbers should always be provided if they exist using the prefix https://doi.org/.

Illustrations/Figures. All illustrative material must be of publication quality. All graphs, drawings and photographs are considered figures and should be kept to a minimum, numbered consecutively with Arabic numerals. Use only solid or open symbols, and avoid the use of light lines or fine screen shading. Distinguish areas within a diagram with solid white or black fill, hatching, or cross-hatching. Figures should be designed to fit one (6.6 cm), one and a half (10.3 cm), or two (13.8 cm) column widths, with a maximum height of 19.6 cm. Figures should be submitted at the size they are to appear in the journal. When reproduced at final size, lettering on figures (capitals and numerals) must be of Arial font and 11 point size. Excel format of graphs are preferred. If figures are made in other programs care must be taken to follow the above instructions in every detail. Figures should be delivered in black and white and will be printed in black and white, but colour printing is possible at the cost of author.

Tables. If results are already given in graphs or diagrams, tables should not be used. Double documentation is not acceptable. Table text should be in ordinary letter size and column headings in bold. Location of figures and tables might be indicated as a comment. Columns or rows within the tables should not be separated with lines. Lining should only be at top and bottom of a table, separating the heading from table content.

Submit your manuscript electronically to the editor at:

editor@ias.is

Editor-in-Chief
Björn Thorsteinsson
Agricultural University of Iceland
Hvanneyri, 311 Borgarnes, Iceland